



Cite this: *Dalton Trans.*, 2016, **45**, 11990

Structural studies of Schiff-base [2 + 2] macrocycles derived from 2,2'-oxydianiline and the ROP capability of their organoaluminium complexes†

Wenxue Yang,^a Ke-Qing Zhao,^a Timothy J. Prior,^b David L. Hughes,^c Abdessamad Arbaoui,^c Mark R. J. Elsegood^d and Carl Redshaw^{*a,b}

The molecular structures of a number of solvates of the [2 + 2] Schiff-base macrocycles {[2-(OH)-5-(R)-C₆H₂-1,3-(CH)₂][O(2-C₆H₄N)₂]}₂ (R = Me **L**¹H₂, tBu **L**²H₂, Cl **L**³H₂), formed by reacting 2,6-dicarboxy-4-R-phenol with 2,2'-oxydianiline (2-aminophenylether), (2-NH₂C₆H₄)₂O, have been determined. Reaction of **L**ⁿH₂ with two equivalents of AlR'₃ (R' = Me, Et) afforded dinuclear alkylaluminium complexes [(AlR'₂)₂**L**¹⁻³] (R = R' = Me (**1**), R = tBu, R' = Me (**2**), R = Cl, R' = Me (**3**), R = Me, R' = Et (**4**), R = tBu, R' = Et (**5**), R = Cl, R' = Et (**6**)). For comparative studies, reactions of two equivalents of AlR'₃ (R' = Me, Et) with the macrocycle derived from 2,2'-ethylenedianiline and 2,6-dicarboxy-R-phenols (R = Me **L**⁴H₂, tBu **L**⁵H₂) were conducted; the complexes [(AlMe)(AlMe₂)**L**⁵]:2½MeCN (**7**·2½MeCN) and [(AlEt₂)₂**L**⁴] (**8**) were isolated. Use of limited AlEt₃ with **L**³H₂ or **L**⁵H₂ afforded mononuclear bis(macrocylic) complexes [Al(**L**³)(**L**³H)]·4toluene (**9**·4toluene) and [Al(**L**⁵)(**L**⁵H)]·5MeCN (**10**·5MeCN), respectively. Use of four equivalents of AlR'₃ led to transfer of alkyl groups and isolation of the complexes [(AlR'₂)₄**L**¹⁻³] (R = **L**², R' = Me (**11**); **L**³, R' = Me (**12**); **L**¹, R' = Et (**13**); **L**², R' = Et (**14**); **L**³, R' = Et (**15**)), where **L**¹⁻³ is the macrocycle resulting from double alkyl transfer to imine, namely {[2-(O)-5-(R)C₆H₂-1-(CH)-3-C(R')H][O(2-(N)-2'-C₆H₄N)₂]}₂. Molecular structures of complexes **7**·2½MeCN, **8**, **9**·4toluene, **10**·5MeCN and **11**·1¼toluene·1¼hexane are reported. These complexes act as catalysts for the ring opening polymerisation (ROP) of ε-caprolactone and *rac*-lactide; high conversions were achieved over 30 min at 80 °C for ε-caprolactone, and 110 °C over 12 h for *rac*-lactide.

Received 18th May 2016,
Accepted 17th June 2016

DOI: 10.1039/c6dt01997h

www.rsc.org/dalton

Introduction

Schiff-base compounds have attracted attention over the years primarily for their biological activity,¹ whilst macrocyclic Schiff bases are of potential interest given their multiple binding sites.² We have been investigating the simplest members of

this Schiff-base macrocyclic family, so-called Robson type macrocycles, derived from the [2 + 2] condensation of a diamine with a dialdehyde, specifically herein 1,3-diformylphenol in combination with the diamine 2,2'-oxydianiline, 2-(2-aminophenoxy)aniline, (2-NH₂C₆H₄)₂O. The structural chemistry of this particular macrocycle is unexplored, indeed a search of the CSD revealed no hits,^{3a} other than our recently reported manganese chemistry.^{3b} Our interest stems primarily from their coordination chemistry and the potential to bind multiple metal centres in close proximity,^{3,4} particularly those which could be of use for ring opening polymerisation (ROP) of cyclic esters to produce biodegradable polymers.⁵ Poly(ε-caprolactone), PCL, and poly(lactide), PLA, are favoured polymers given both their biodegradability, and that their copolymers are considered as potential environmentally friendly commodity plastic.⁶ Given the central role played by metal-complex induced coordination/insertion type ROP processes, investigations into new combinations of metals and ancillary ligands are pivotal when trying to identify structure–activity relationships. Indeed, in previous work,^{4a} we communicated

^aCollege of Chemistry and Materials Science, Sichuan Normal University, Chengdu, 610066, China. E-mail: C.Redshaw@hull.ac.uk

^bDepartment of Chemistry, University of Hull, Hull, HU6 7RX, UK

^cSchool of Chemistry, University of East Anglia, Norwich, NR4 7TJ, UK

^dChemistry Department, Loughborough University, Loughborough, Leicestershire, LE11 3TU, UK

† Electronic supplementary information (ESI) available: X-ray crystallographic files CIF format for the structure determinations of compound **L**¹H₂·MeCN, **L**²H₂·MeCN, **L**²H₂·2(Me₂CO) and **L**²H₂·*n*(MeCOOEt), *n* = 1 and 2, **L**²H₂·2(PhMe), **L**²(tosyl)₂, **7**·2½MeCN, **8**, **9**·4toluene, **10**·5MeCN and **11**·1¼toluene·1¼hexane. Alternative views of structures and further polymerisation data. CCDC 1442772–1442778 (Schiff-base pro-ligands) and 1463685–1463689 (organoaluminium complexes). For ESI and crystallographic data in CIF or other electronic format see DOI: 10.1039/c6dt01997h



how remote alkylaluminium centres bound to a Schiff-base macrocycle derived from the dianiline $[(\text{CH}_2\text{CH}_2)(2\text{-C}_6\text{H}_4\text{NH}_2)_2]$ exhibited beneficial cooperative effects in the ROP of ϵ -caprolactone, whereas the presence of aluminoxane type (Al–O–Al) bonding proved detrimental. Given this, we have re-focused our efforts on such Schiff-base systems and have extended our studies to $[2 + 2]$ macrocycles derived from the dianiline $(2\text{-NH}_2\text{C}_6\text{H}_4)_2\text{O}$ (see Chart 1). Herein, we report the molecular structures of a number of these $[2 + 2]$ macrocycles, and find that they tend to adopt a taco-like, folded conformation. Interestingly, a series of zinc complexes bearing phenol compartmental type ligation were recently found to exhibit controllable photophysical properties by manipulation of the substituent (Me, *t*Bu, Cl) positioned *para* to the phenolic group.⁷

Furthermore, we have investigated the reaction chemistry of L^{1-3}H_2 towards the alkylaluminium reagents R_3Al (R = Me, Et) and have isolated some unexpected products (Chart 1). Given this, related studies on macrocycles derived from the ethylene-bridged dianiline $[(\text{CH}_2\text{CH}_2)(2\text{-C}_6\text{H}_4\text{NH}_2)_2]$ were conducted,

and the ability of these complexes to act as catalysts for the ring opening polymerisation (ROP) of ϵ -caprolactone and *rac*-lactide has been investigated. The use of alkylaluminium complexes for the ROP of cyclic esters has recently been reviewed.⁸

Results and discussion

Preparation, structure and emission studies on L^nH_2

The $[2 + 2]$ Schiff base macrocycles of type L^nH_2 are readily available in high yield *via* the reaction of 2,6-dicarboxy-4-R-phenol, where R = Me ($n = 1$), *t*Bu ($n = 2$) or Cl ($n = 3$), with 2,2'-oxydianiline, $(2\text{-NH}_2\text{C}_6\text{H}_4)_2\text{O}$. In the IR spectra, $\nu(\text{C}=\text{N})$ for L^1H_2 (1626 cm^{-1}), L^2H_2 (1630 cm^{-1}) and L^3H_2 (1627 cm^{-1}) bands are strong and are very similar to those reported for related ethylene ($-\text{CH}_2\text{CH}_2-$) bridged bis(imino)phenoxide macrocycles ($1627\text{--}1629\text{ cm}^{-1}$),^{3b,4} and also lie within the range reported for other Schiff-base macrocycles.⁹ In the

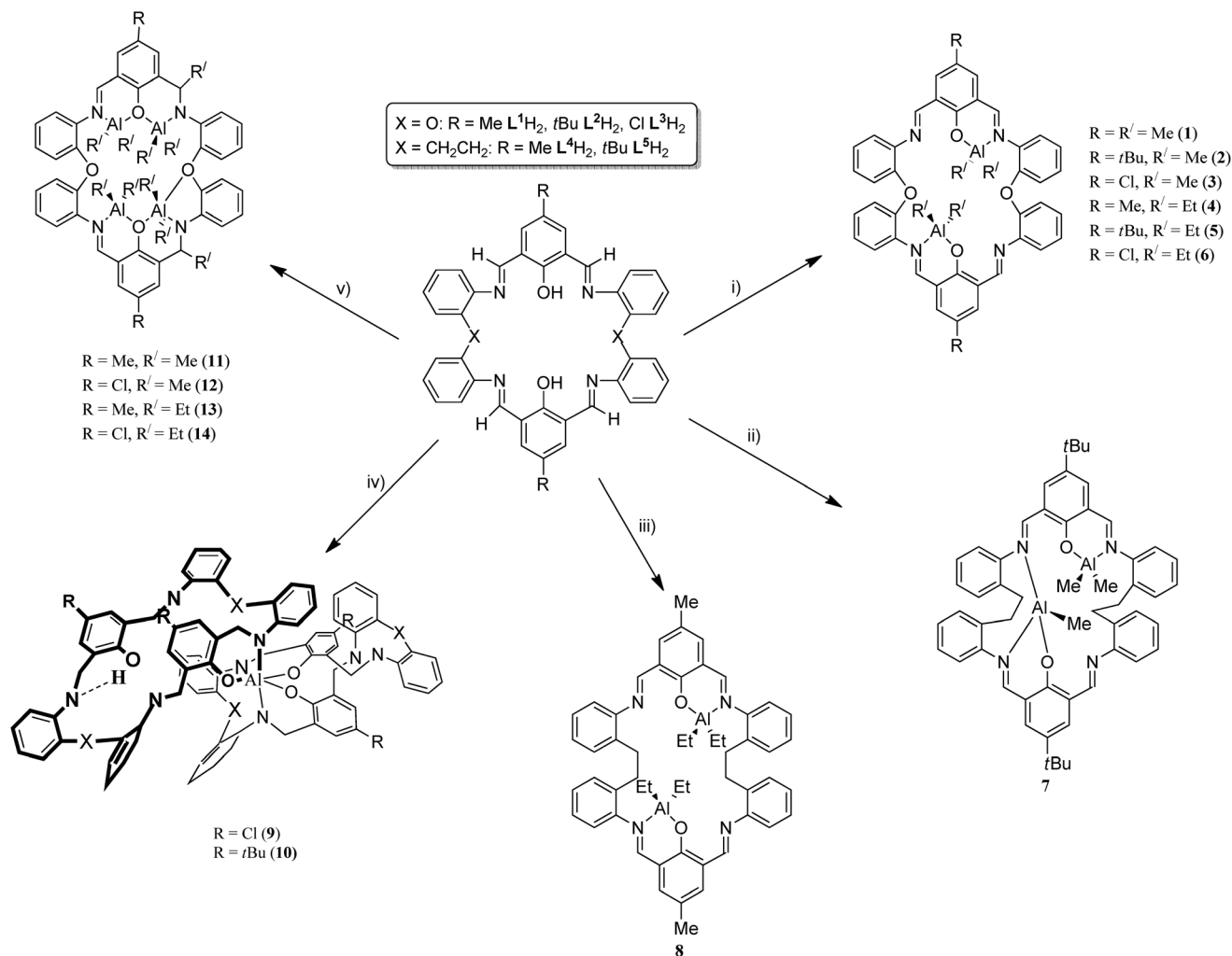


Chart 1 Synthesis of aluminium complexes 1–14 prepared herein. Reagents and conditions: (i) $2\text{R}_3\text{Al}$, hexane, Δ , 12 h; (ii) $2\text{Me}_3\text{Al}$, toluene, Δ , 12 h; (iii) $2\text{Et}_3\text{Al}$, toluene, Δ , 12 h; (iv) $\frac{1}{2}\text{Et}_3\text{Al}$, hexane, Δ , 12 h; (v) $4\text{R}_3\text{Al}$, hexane, Δ , 12 h.



^1H NMR spectra, the imino hydrogen chemical shifts for L^2H_2 (8.40 ppm) and L^3H_2 (8.43 ppm) are comparable with those reported previously for bis(imino)phenol-based macrocycles [8.12 to 8.66 ppm],¹⁰ whilst that for L^1H_2 (8.87 ppm) is shifted slightly downfield.

These condensation products $\{[2-(\text{OH})-5-(\text{R})\text{C}_6\text{H}_2-1,3-(\text{CH})_2][(\text{O})(2-\text{C}_6\text{H}_4\text{N})_2]\}_2$ ($\text{R} = \text{Me } \text{L}^1\text{H}_2, t\text{Bu } \text{L}^2\text{H}_2, \text{Cl } \text{L}^3\text{H}_2$) can be recrystallized from a variety of solvents; the molecular structures of a number of solvates are described below. Selected bond lengths and angles for each of the solvates are either discussed in the text or, in the case of L^2H_2 , are presented in Table 1, with crystallographic parameters for all structures collated in Table 5. In each case, crystals of L^nH_2 suitable for an X-ray diffraction study were grown from the respective solvent on prolonged standing at ambient temperature. The molecular structure of $\text{L}^1\text{H}_2\cdot\text{MeCN}$ is shown in Fig. 1. In the asymmetric unit, there is one macrocycle and one molecule of MeCN. The macrocycle adopts an open, taco-like conformation, and the orientation of the two sides of the macrocycle can be monitored by looking at the cleft angle ϕ (ϕ is defined as the angle subtended between the mean planes of the two phenolate rings (O1 C1–C6, C8, C42, N1, N4 and C21–C27, C29, N2, N3, O3) as illustrated in Fig. 2). Thus, the smaller the cleft angle, the more parallel are the sides and the more taco-like the conformation. In the case of $\text{L}^1\text{H}_2\cdot\text{MeCN}$, the open-taco description reflects the approximate cleft angle of 89.2° . A more detailed analysis of the orientation of the rings is presented in Table S1 (see ESI[†]). The MeCN molecule is encapsulated by the macrocycle between the rings incorporating C19 and C43. The centroid-to-centroid distance is approximately 8.5 Å, whilst the shortest $\text{H}_{(\text{MeCN})}$ to centroid distances are 3.76 and 3.66 Å. The closest neighbour of the MeCN methyl group is the phenolic group with $\text{O1}\cdots\text{H52c}$ at 2.51 Å. The compound displays strong intramolecular hydrogen bonds involving the phenolic hydrogen and an imino nitrogen [$\text{H1}\cdots\text{N1} = 1.74(3)$ Å and $\text{H3}\cdots\text{N3} = 1.59(3)$ Å; $\text{O1-H1}\cdots\text{N1} = 150(3)^\circ$ and $\text{O3-H3}\cdots\text{N3} = 152(3)^\circ$].

Intermolecular face-to-face interactions give rise to stacks along the c direction (see Fig. S1, ESI[†]).

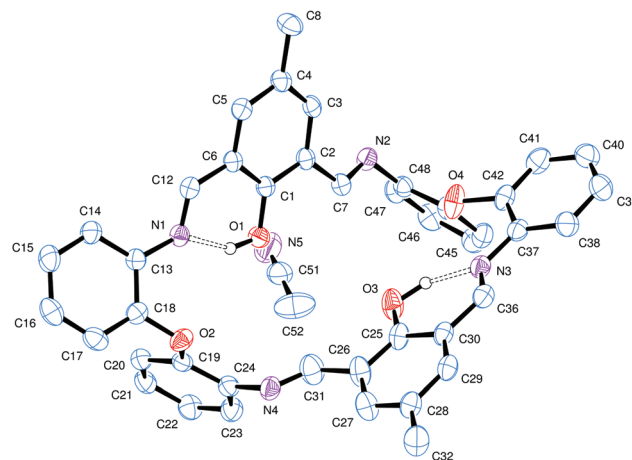


Fig. 1 Molecular structure of $\text{L}^1\text{H}_2\cdot\text{MeCN}$. Selected bond lengths (Å) and angles ($^\circ$): N1–C12 1.284(2), N1–C13 1.415(2), N2–C7 1.276(2), N2–C48 1.419(2); C6–C12–N1 121.50(13), C2–C7–N2 121.44(14). H atoms not involved in H-bonding are omitted for clarity.

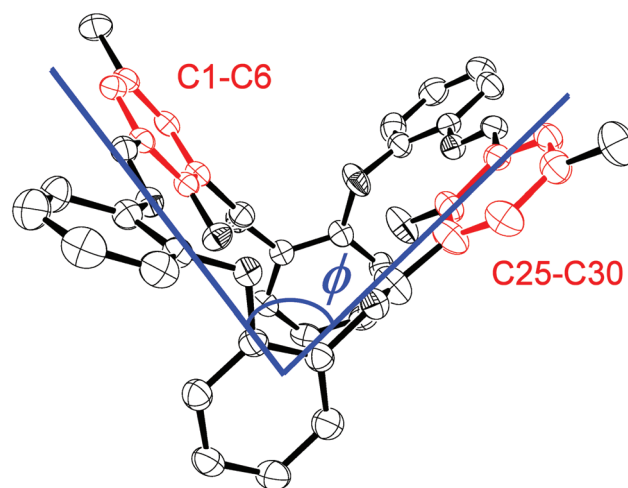


Fig. 2 The cleft ϕ , defined by the angle subtended by the mean planes of the phenolic rings.

Table 1 Comparison of selected geometrical parameters for solvates of L^2H_2

	$\text{L}^2\text{H}_2\cdot\text{MeCN}$	$\text{L}^2\text{H}_2\cdot\text{EtOAc}$	$\text{L}^2\text{H}_2\cdot 2\text{acetone}$	$\text{L}^2\text{H}_2\cdot 2\text{toluene}$
N1–C12	1.286(3)	1.288(2)	1.280(2)	1.282(3)
N1–C13	1.412(3)	1.4188(19)	1.4112(18)	1.415(3)
N2–C7	1.258(3)	1.2679(19)	1.2616(19)	1.276(3)
N2–C24'/48	1.411(3)	1.412(2)	1.417(2)	1.422(3)
C18–O2	1.395(3)	1.3971(19)	1.385(2)	1.392(3)
O2–C19	1.401(3)	1.4022(19)	1.398(2)	1.391(3)
C18–O2–C19	116.3(2)	115.40(11)	117.10(12)	116.45(19)
C12–N1–C13	123.2(3)	119.70(13)	121.71(15)	120.45(19)
N2–C7–C2	122.5(3)	121.67(14)	123.80(16)	122.6(2)
N1–C12–C6	120.0(3)	122.75(14)	121.78(15)	121.4(2)
C14–C13–N1	126.1(3)	123.87(14)	124.09(15)	124.1(2)
C18–C13–N1	116.0(3)	118.50(14)	117.58(15)	117.1(2)
C7–N2–C24'/48	116.6(3)	119.29(14)	116.98(15)	117.05(19)



In the case of $L^2H_2 \cdot MeCN$, there are two very similar, independent molecules in the asymmetric unit, together with two molecules of solvent (MeCN), both of which are disordered in several orientations. In this case, the conformation in each macrocyclic molecule is much more closed with ϕ angles of about 13 and 15°, *i.e.* the two sides of the cleft are almost parallel. The whole molecule shows approximate symmetry about a pseudo two-fold axis (see Fig. S2 and S3†). The pseudo symmetry axes of the two molecules are not parallel. Distinct from $L^1H_2 \cdot MeCN$, the solvent does not reside in a pocket and has no close interaction with the macrocyclic ring. As expected, the bond lengths in $L^2H_2 \cdot MeCN$ are similar to those observed in $L^1H_2 \cdot MeCN$, and in each molecule of $L^2H_2 \cdot MeCN$, the hydroxyl hydrogen atoms of the phenol groups were all located from difference maps and refined well to show clear intramolecular hydrogen bonding with neighbouring imine nitrogen atoms [molecule 1: H10–N1 = 1.57(3) Å and O1–H10...N1 = 150(3)°, H30–N3 = 1.79(3) Å and O3–H30...N3 = 148(3)°; molecule 2: H510–N51 = 1.68(3) Å and O1–H510...N51 = 148(3)°, H530–N53 = 1.64(3) Å and O3–H530...N53 = 150(3)°].

L^2H_2 can also be readily crystallized from ethyl acetate from which two different solvates were isolated on separate occasions. The molecular structure of one product is shown in Fig. S4 (ESI†), with selected bond lengths and angles given in Table 1. The asymmetric unit contains half a molecule of L^2H_2 and half a disordered solvent molecule. The second half of the macrocycle molecule is generated by a two-fold symmetry axis. Again, the macrocycle possesses quite a tight cleft angle ϕ at about 17°. As in the previous solvates, there is intramolecular H-bonding involving the phenolic hydrogen and an imino nitrogen [H10–N1 = 1.75(2) Å and O1–H10...N1 = 153(2)°]. The disordered ethyl acetate solvent molecule resides over an inversion centre, and is located in a pocket between four of the macrocycles.

A separate crystallization afforded a different solvate, namely $L^2H_2 \cdot 2(\text{ethyl acetate})$, the asymmetric unit for which (not shown) contains half a molecule of the macrocycle and one solvent molecule. The main difference from the mono-solvate is that there is a pronounced twist about the central bond, resulting in a C12–N1–C13–C14 torsional angle of –33.1(8)° (the same angle in the mono-solvate is –15.8(2)°). The ϕ angle of the V-shaped cleft in $L^2H_2 \cdot 2(\text{ethyl acetate})$ is about 7° (*i.e.* close to parallel), though it should be noted here that the distance between the rings of each side of the cleft (see Fig. S5, ESI†) is larger than in the mono-solvate, with a mean of 3.7 Å (*cf.* 3.5 Å for the mono-solvate).

In the case of the crystallization from acetone, the asymmetric unit contains half a macrocycle and one molecule of acetone. A similar conformation (Fig. S6, ESI†) to the ethyl acetate solvate is adopted in that the V-shaped cleft has a very tight ϕ angle (*ca.* 8°). Pairs of acetone molecules, arranged centrosymmetrically, reside in approximately spherically shaped pockets formed between the macrocycle molecules. Again, there is intramolecular H-bonding involving the phenolic hydrogen and an imino nitrogen [H10–N1 = 1.68(2) Å and O1–H10...N1 = 151(2)°].

The two different ethyl acetate solvates and the acetone solvate all crystallize in similar sized and shaped unit cells in space group $C2/c$; *i.e.* they are almost isomorphous (see Table 5 for unit cell geometry).

For the toluene solvate (Fig. S7, ESI† and Table 1), the asymmetric unit contains a single macrocycle and two unique solvent molecules. In this case, the conformation adopted by the macrocycle is more open such that the ‘cleft’ has an approximate ϕ angle of 89°. This open conformation allows for the formation of intermolecular $\pi \cdots \pi$ and $CH \cdots \pi$ interactions. The phenyl rings do not directly overlay, rather they are somewhat slipped such that a C–C bond in one ring is positioned directly below the centroid of an adjacent ring (see Fig. S8, ESI†). The shortest C to centroid distances are 3.38 and 3.42 Å. Intramolecular H-bonding is present involving the phenolic hydrogen and an imino nitrogen [H10–N1 = 1.74(3) Å and O1–H10...N1 = 150(3)°, H30–N3 = 1.66(3) Å and O1–H30...N3 = 151(3)°].

In these solvates, the range of C=N bond lengths (1.258(3)–1.288(2) Å, see Table 1 and caption for Fig. 1) compares favourably with those reported for the related ethylene bridged phenolic macrocycles [1.2554(17)–1.299(7) Å],^{4b} and those observed in bis(imino)pyridine containing macrocycles [1.246(3)–1.289(3) Å].¹¹

In these L^2H_2 derived systems, the angular variation in the V-shaped cleft can also be gauged by the gradation of tilting of the *t*-butyl-phenol groups, from 6.09(8)° in $L^2H_2 \cdot MeCOOEt$, through $L^2H_2 \cdot 2(MeCOOEt)$ at 6.8(2)°, $L^2H_2 \cdot 2(\text{acetone})$ at 7.39(7)°, $L^2H_2 \cdot MeCN$ at 9.49(14) and 12.56(12)° in the two molecules (for further analysis see Table S1, ESI†). By contrast, for the L^1H_2 system, the structure is more open, for example $L^1H_2 \cdot MeCN$ at 89.03(5)°. $L^2H_2 \cdot 2(\text{toluene})$ is also more open, at 89.88(7), and in $L^2(\text{tosyl})_2$, where the two phenolate rings are opposed and related by a centre of symmetry, the angle is 180.0°.

Tosylated macrocycle

The precursor 2,6-dicarboxy-4-R-phenol was prepared *via* tosylation of the parent tris(hydroxyl) compound 2,6-dimethanol-4-R-phenol, and during these syntheses, we isolated one of the tosylated intermediates, which was subsequently reacted with oxydianiline. The resulting tosylated macrocycle $L^2(\text{tosyl})_2$ was crystallized from acetonitrile. The molecular structure is shown in Fig. S9, ESI (and an alternative view is given in Fig. S10 in the ESI†), with selected bond lengths and angles given in the caption. There is half a molecule in the asymmetric unit, and the molecule lies on an inversion centre. In the packing of the molecules, there is off-set $\pi \cdots \pi$ stacking: C1...C2' = 3.700 Å, C2...O1' = 3.456 Å and C6...C7' = 3.684 Å.

Preparation, structure and ROP behaviour of organoaluminium complexes

The reaction of the [2 + 2] macrocyclic Schiff bases $\{[2-(OH)-5-(R)C_6H_2-1,3-CH][O(2-C_6H_4N)_2]\}_2$ (R = Me L^1H_2 , *t*Bu L^2H_2 , Cl L^3H_2) with two equivalents of R'_3Al in refluxing hexane afforded, following work-up, cooling and prolonged standing



(1–2 days) at ambient temperature, yellow crystals in good yield (*ca.* 55–67%) of the dinuclear complexes $[(AlR'_2)_2L]$ (L^1 , $R' = Me$ (1), L^2 , $R' = Me$ (2), L^3 , $R' = Me$ (3), L^1 , $R' = Et$ (4), L^2 , $R' = Et$ (5), L^3 , $R' = Et$ (6)). Unfortunately, we were unable to grow single crystals of 1–6 suitable for X-ray crystallography, and so our attention turned to systems derived from the ethylene-bridged dianiline $[(CH_2CH_2)(2-C_6H_4NH_2)_2]$ prepared under the same conditions. In previous work, we have investigated the reaction of two equivalents of R'_3Al with such $[2 + 2]$ Schiff-base macrocycles, but no structural information was reported. Herein, for $R' = Me$, we were able to isolate and structurally characterize a secondary product, namely $[(AlMe)(AlMe_2)L^3] \cdot 2\frac{1}{4}MeCN$ (7). Small, orange, plate-like crystals were grown from a saturated acetonitrile solution on prolonged standing at ambient temperature. The crystals proved to be weakly diffracting, even when using synchrotron radiation, and so data was only integrated to $2\theta = 45^\circ$. The asymmetric unit contains two macrocyclic complexes and 4.5 molecules of solvent of crystallization (MeCN). The molecular structure of one of the macrocyclic structures is shown in Fig. 3, with selected bond lengths and angles given in the caption. The interesting features of this complex are (i) the different degree of alkylation of the distorted tetrahedral aluminium centres, with Al1 bearing two methyl groups, whereas Al2 has only one, and (ii) the 'trans' positioning of the Al1 centres. Thus for Al1, the macrocycle binds in *N,O*-bi-dentate fashion, whereas for Al2, the macrocycle coordinates *via* a tri-dentate *N,N,O* mode. The conformation of the macrocycle is somewhat twisted to accommodate the tridentate nature of the bonding at Al2.

Given the unexpected nature of complex 7, we re-visited the complex $\{[Et_2Al][2-(O)-5-(Me)C_6H_2-1,3-CH][CH_2CH_2(2-C_6H_4N)_2]\}_2$ (8) and determined the centro-symmetric molecular structure

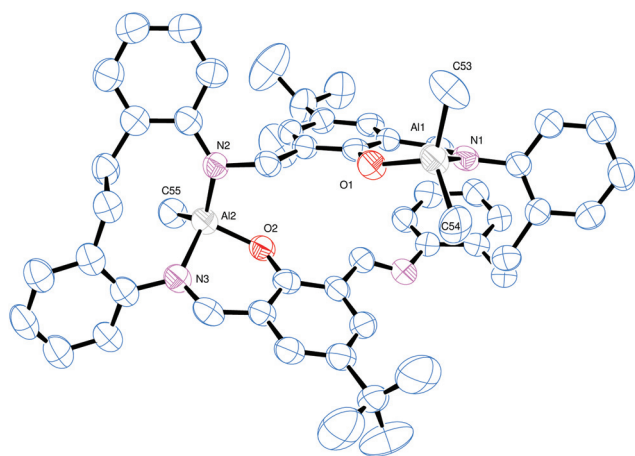


Fig. 3 Molecular structure of $[(AlMe)(AlMe_2)L^3] \cdot 2\frac{1}{4}MeCN$ (7, $R = tBu$) (7), with atoms drawn as 50% probability ellipsoids. Hydrogen atoms and MeCN of crystallisation have been omitted for clarity. This is one of two similar macrocyclic complexes in the asymmetric unit. Selected bond lengths (Å) and angles ($^\circ$): Al1–O1 1.761(4), Al1–N1 1.963(5), Al1–C53 1.977(6), Al1–C54 1.949(5), Al2–O2 1.768(4), Al2–N2 1.860(4), Al2–N3 1.970(4), Al2–C55 1.963(5); O1–Al1–N1 94.49(17), C53–Al1–C54 119.3(3), N2–Al2–N3 110.90(18), O2–Al2–C55 109.2(2).

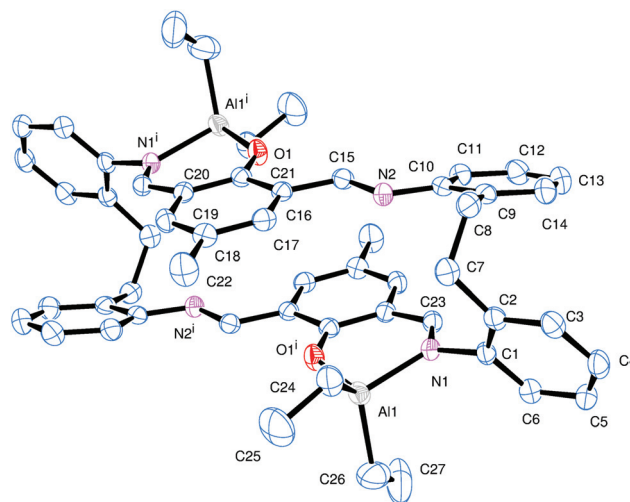


Fig. 4 Molecular structure of $[(AlEt_2)_2L^4]$ (8), with atoms drawn as 50% probability ellipsoids. Symmetry operator used to generate the second half of the molecule: $i = 1 - x, -y, 1 - z$. Hydrogen atoms and MeCN of crystallisation have been omitted for clarity. Selected bond lengths (Å) and angles ($^\circ$): Al1–N1 1.9710(16), Al1–O1ⁱ 1.7826(13), N1–C23 1.294(2), N12–C15 1.276(2); N1–Al1–O(1ⁱ) 94.67(6), N1–Al1–C26 106.37(10).

of crystals grown from a saturated acetonitrile solution, see Fig. 4 and Table 6. Interestingly, again the structure reveals a 'trans' deposition of the distorted tetrahedral aluminium centres, though in this case there is the anticipated diorgano-aluminiums present. Each is bound to the two opposite phenolic oxygen atoms and to a neighbouring imine nitrogen (N1 or N1ⁱ). The conformation of the macrocycle is relatively planar. The observed 'trans' deposition of the diethylaluminium centres in 8 could be explained in terms of steric effects, but the situation in 7 is less clear.

Conducting the reaction of L^3H_2 with limited Et_3Al resulted in the isolation of a yellow crystalline material. Crystals grown from a saturated solution of toluene were found to be a bis-chelate structure $[Al(L^3)(L^3H)] \cdot 4toluene$ (9·4toluene) (see Fig. 5,

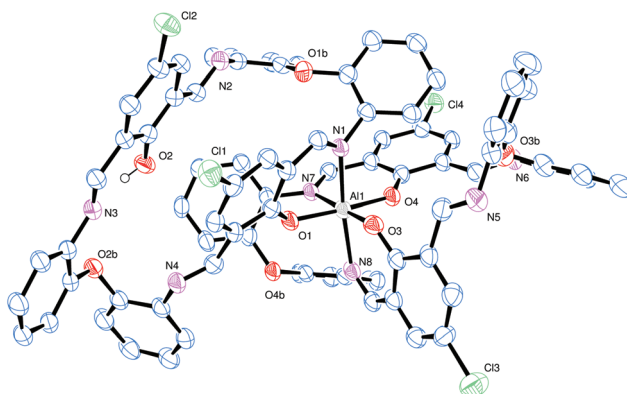


Fig. 5 View of the molecular structure of $[Al(L^3)(L^3H)] \cdot 4toluene$ (9·4toluene), with atoms drawn as 50% probability ellipsoids. Hydrogen atoms, except that on O2 which H-bonds to N3, and toluene molecules of crystallisation have been omitted for clarity.



Table 2 Selected structural data for **9-4toluene** and **10-5MeCN**

Bond length (Å)/angle (°)	9-4toluene	10-5MeCN
Al1–O1	1.8121(17)	1.814(3)
Al1–O3	1.8410(17)	1.819(3)
Al1–O4	1.8338(17)	1.817(3)
Al1–N1	2.100(2)	2.090(3)
Al1–N7	2.079(2)	2.112(4)
Al1–N8	2.114(2)	2.087(3)
O1–Al1–O4	176.18(8)	173.51(16)
O3–Al1–N7	176.96(8)	178.76(14)
N1–Al1–N8	168.76(8)	173.02(15)

Tables 2 and 6), in which a distorted octahedral aluminium centre is bound to two of the macrocyclic ligands.

The asymmetric unit contains one complex and four toluene molecules. The central octahedral Al centre is bound by two macrocycles, with one of the macrocycles binding through two atoms [O1 and N1] to form a nearly planar 6-membered chelate ring; the remainder of this macrocycle adopts a taco-like configuration. The remaining coordination sites at aluminium are occupied by two pairs of O/N chelators (both from the other macrocycle), again forming six membered rings that are close to planar. These two chelate rings are linked by a phenyl ring and a single oxo bridge, and are approximately perpendicular at the aluminium. The remainder of this macrocycle adopts a bowl-shaped conformation. There is a single O–H...N hydrogen bond formed by the unbound phenol present. Within the solid-state, the crystal packing facilitates a large number of non-classical C–H...N and C–H...Cl hydrogen bonds. Four unique, crystallographically resolved, toluene molecules lie between the complexes. There is rotational disorder in their positions but no regions of disordered solvent that could be resolved. There is evidence that C–H... π interactions help to locate the toluene.

Similar treatment of L^5H_2 again afforded a bis-chelate structure, namely $[Al(L^5)(L^5H)] \cdot 5MeCN$ (**10-5MeCN**), for which single crystals suitable for X-ray diffraction were grown from toluene at 0 °C.

The molecular structure of **10-5MeCN** is shown in Fig. 6 and S11 and S12 (ESI[†]) which, along with the geometrical parameters

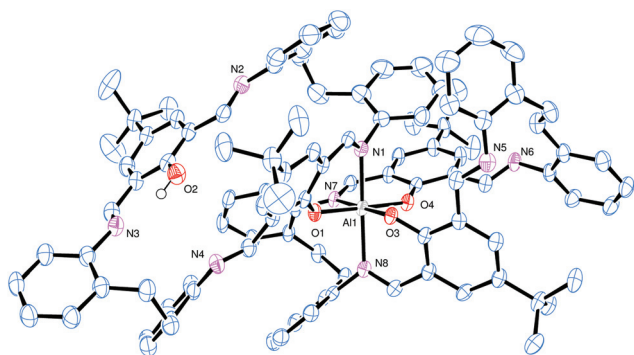


Fig. 6 The molecular structure of $[Al(L^5)(L^5H)] \cdot 5MeCN$ (**10-5MeCN**), with atoms drawn as 50% probability ellipsoids. Hydrogen atoms, except that on O2 which H-bonds to N3, and MeCN solvent molecules of crystallisation have been omitted for clarity.

(Table 2), reveals the similarity between complexes **9-4toluene** and **10-5MeCN**. The asymmetric unit contains one aluminium complex and 5 molecules of acetonitrile. As for **9-4toluene**, the coordination at the aluminium is such that one macrocycle is bound only in chelate fashion *via* *N,O*-type ligation, whilst the second macrocycle utilizes four atoms to bind in $2 \times N,O$ -type fashion. In the bidentate ligand, there is also an intramolecular H-bond involving the phenolic group at O2 and the adjacent imine nitrogen N3. In terms of packing, the aromatic ring at C38 forms a centrosymmetric $\pi \cdots \pi$ interaction at 3.6 Å.

Treatment of LH_2 with excess R'_3Al (four equivalents) in refluxing hexane afforded, following work-up (extraction into toluene), cooling and prolonged standing (1–2 days) at ambient temperature, yellow crystals in moderate yield (*ca.* 30–35%) of the tetra-nuclear complexes $[(AlR'_2)_4L^{1'-3'}]$ ($R = L^2$, $R' = Me$ (**11**); L^3 , $R' = Me$ (**12**); L^1 , $R' = Et$ (**13**); L^3 , $R' = Et$ (**14**)), where $L^{1'-3'}$ is the macrocycle resulting from double alkyl transfer to imine, namely $\{[2-(O)-5-(R)C_6H_2-1-(CH)-3-C(R'H)][(O)(2-(N)-2'-C_6H_4N)_2]\}_2$. In the case of the reaction involving L^1H_2 and Me_3Al , single crystals of the complex were grown from a saturated hexane/toluene (50 : 50) solution at 0 °C. The molecular structure is shown in Fig. 7, with selected bond lengths

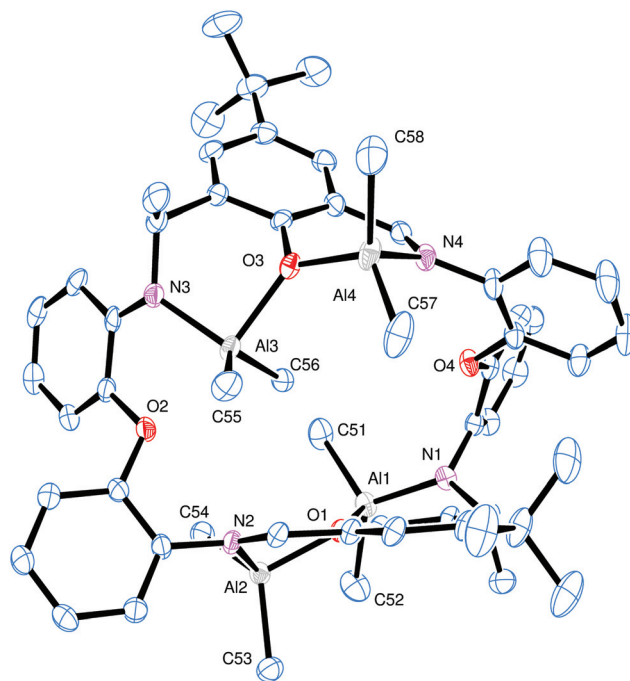


Fig. 7 Molecular structure of $[(AlMe_2)_4L^1] \cdot 1\frac{1}{2}toluene \cdot 1\frac{1}{2}hexane$ (**11-1 $\frac{1}{2}$ toluene-1 $\frac{1}{2}$ hexane**), showing the atom numbering scheme. Hydrogen atoms and solvent molecules of crystallisation have been omitted for clarity. This is one of four unique complex molecules in the asymmetric unit. Selected bond lengths (Å) and angles (°): Al1–N1 1.820(3), Al1–O1 1.950(2), Al2–O1 1.857(2), Al2–N2 1.952(2), Al3...O2 2.430(2), Al3–O3 1.997(2), N1–C1 1.469(4), N2–C13 1.286(4), N2–C15 1.276(2), N2–C14 1.442(4), N3–C25 1.381(4), N3–C26 1.473(4), N4–C38 1.288(4), N4–C39, Al1...Al2 3.1695(12), Al1...Al3 5.8984(13), Al1...Al4 7.3100(13), Al2...Al3 5.0994(13), Al2...Al4 7.5339(13), Al3...Al4 3.4600(13); Al1–O1–Al2 112.73(10), Al3–O3–Al4 129.79(12), N1–Al1–O1 95.53(10), O1–Al2–N2 94.72(10).



and angles given in the caption. This reveals the formation of a tetra-nuclear complex (**11**) akin to that formed from when using the analogous $-\text{CH}_2\text{CH}_2-$ bridged Schiff-base macrocycle.¹² For a relatively simple compound, the crystal structure displays unwelcome complexity. There are four, symmetry unique, bowl-shaped molecules of $11 \cdot 1\frac{3}{4}\text{toluene} \cdot 1\frac{1}{2}\text{hexane}$ occupying the asymmetric unit. Each of these binds four AlMe_2 units; subtle differences in the configuration of the macrocycles render these symmetry independent. Between these macrocycles lie crystallographically resolved and unresolved solvent to give an estimated formula (after Squeeze)¹³ of $8\{(\text{Me}_2\text{Al})_4[2-(\text{O})-5-(t\text{Bu})\text{C}_6\text{H}_2-1-\text{CH}-3\text{C}(\text{Me})\text{H}][\text{O}(2-\text{C}_6\text{H}_4\text{N})_2]\}_2 \cdot 14\text{toluene} \cdot 9\text{hexane}$. To simplify the discussion of the four similar units, the orientation of one macrocycle will be discussed. The macrocycle is twisted such that one *tert*-butyl group is pointing 'up' and one 'down'. At the opposite end of each of the phenyl groups bearing the *tert*-butyl are bound two AlMe_2 units. Each aluminium is coordinated by two methyl groups and one neutral imine and a phenoxide in approximately tetrahedral geometry. The phenoxides bridge between the two aluminium centres (atoms O1 and O3 in Fig. 7). One pair of aluminium atoms reside on one side of the molecule and the others lie on the opposite side. There is evidence for $\text{C}-\text{H} \cdots \pi$ interactions between adjacent macrocycles but the packing is unremarkable. Between the macrocycles lie ordered and disordered solvent; some hexane and toluene are crystallographically resolved. There are also portions of the structure in which the solvent molecules cannot be located reliably and these regions were modelled using the Squeeze routine.¹³

The formation of **11** involves an intramolecular regioselective methyl transfer to two imine moieties of the macrocycle; such methyl transfers are now well established in imine chemistry.¹⁴ The methyl transfer occurs at imine groups orig-

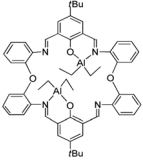
inating from the same dianiline. In the ^1H NMR spectra of **11**, the $\text{Me}-\text{Al}$ resonances occur as eight singlets between -0.52 and -1.39 ppm (and four singlets between -0.49 and -1.01 for **12**). In the case of the related ethyl derivatives **13** and **14**, two of the $\text{Al}-\text{Et}$ groups appear to be subject to ring currents which result in unusual low field chemical shifts in the ^1H NMR spectra for the CH_2 protons (see Experimental section).

Ring opening polymerisation (ROP) of ϵ -caprolactone and *rac*-lactide

The dinuclear alkylaluminium complexes **1-6** and the tetra-nuclear alkylaluminium complexes **11-14** have been screened for their ability to ring open polymerise ϵ -caprolactone (see Tables 3 and S2†) and *rac*-lactide (Tables 4 and S4†). Results are compared against the known $-\text{CH}_2\text{CH}_2-$ bridged complexes **15** and **16**.

ROP of ϵ -caprolactone. Runs were conducted both in the presence and absence of benzyl alcohol (BnOH). Complex **5** was used to determine the optimized conditions (Table 3). On increasing the temperature from 20 to 110 °C and using 250 : 1 : 1 (ϵ -CL : cat : BnOH) over 30 min (runs 1-4, Table 3), the % conversion dramatically increased, reaching around 98% conversion at 80 °C and then increasing only slightly on further elevating the temperature to 110 °C. Under the same conditions, the molecular weight (M_n) peaked at 80 °C. All the polycaprolactone polymers (PCLs) obtained possessed a narrow distribution/polydispersity index (PDI) with unimodal characteristics [$M_w/M_n = 1.12-1.58$]. The drop off in molecular weight at 110 °C results in a plot of % conversion *versus* M_n which is only approximately linear. We have also investigated the effect of the ϵ -CL/Al molar ratio on the catalytic behaviour (entries 3, 8 and 9, Table 3) in the presence of one equivalent of BnOH. When the molar ratio CL : Al was increased from 100 to 500 over 30 min, the molecular weight increased from 2.16

Table 3 ROP of ϵ -CL using complex **5**



Run	Cat.	CL : Al : BnOH	$T/^\circ\text{C}$	t/min	Conv. ^a /%	$M_n \times 10^4$ ^b	$M_{n,\text{Calcd}} \times 10^4$ ^c	PDI
1	5	250 : 1 : 1	20	60	15.8	0.59	0.45	1.08
2	5	250 : 1 : 1	50	30	64.4	1.57	1.82	1.15
3	5	250 : 1 : 1	80	30	98.0	3.36	2.82	1.56
4	5	250 : 1 : 1	110	30	98.5	2.67	2.71	1.58
5	5	250 : 1 : 1	80	10	59.0	2.98	1.68	1.29
6	5	250 : 1 : 1	80	20	92.5	3.24	2.63	1.34
7	5	250 : 1 : 1	80	60	99.2	2.88	2.69	1.40
8	5	100 : 1 : 1	80	30	99.1	2.16	1.12	1.13
9	5	500 : 1 : 1	80	30	86.7	4.62	4.94	4.01
11	5	250 : 1 : 0	80	30	80.1	6.59	2.28	1.60
12	5	250 : 1 : 3	80	30	93.1	2.02	2.65	1.26

^a By ^1H NMR spectroscopic analysis. ^b Obtained from GPC analysis times 0.56. ^c $(F.W.[M]/[BnOH])(\text{conversion})$.



Table 4 ROP of *rac*-lactide using complex 5

Run	Lac : M : BnOH	T/°C	t/h	Conv. ^a /%	$M_n \times 10^4$ ^b	$M_{n,Cal} \times 10^4$ ^c	PDI
1	100 : 1 : 1	110	1	57.8	0.42	0.83	1.02
2	100 : 1 : 1	110	3	91.3	0.63	1.31	1.03
3	100 : 1 : 1	110	6	95.0	1.56	1.39	1.21
4	100 : 1 : 1	110	12	97.7	1.60	1.40	1.19
5	100 : 1 : 1	110	24	98.6	1.45	1.40	1.14
6	100 : 1 : 1	50	12	—	—	—	—
7	100 : 1 : 1	80	12	66.7	0.74	0.96	1.07
8	50 : 1 : 1	110	12	94.3	0.80	0.67	1.41
9	200 : 1 : 1	110	12	96.6	2.29	2.78	1.14

^a By ¹H NMR spectroscopic analysis. ^b M_n values were determined by GPC in THF vs. PS standards and were corrected with a Mark-Houwink factor of 0.58. ^c Polydispersity index (M_w/M_n) were determined by GPC.

to 4.62×10^4 , whilst the conversion rate exhibited the opposite trend peaking at 99.1% for 100 : 1 : 1; the molecular weight distribution increased on increasing the molar ratio CL : Al (from 1.13 to 4.01). On increasing the time from 10 min to 60 min, and using 250 : 1 : 1 (CL : Al : BnOH) at 80 °C (runs 3, 5–7, Table 3), the conversion gradually increased with time, whilst the molecular weight (M_n) and polydispersity (PDI) remained relatively constant, except in the case of run 9 where it was, surprisingly, somewhat broader (4.01). Increasing the amount of BnOH (run 12 *versus* 3, Table 3) was detrimental to the molecular weight (M_n), whilst only slightly narrowing the polydispersity, and lowering the % conversion slightly. Conducting the ROP in the absence of BnOH (run 11 *versus* 3, Table 3) led to a reduction in the % conversion, but afforded a significant increase in the polymer molecular weight (M_n); there was little change in the PDI.

Complexes 1–14 (not 8–10) were then screened using the ratio 250 : 1 : 1 (ϵ -CL : cat : BnOH) over 30 min at 80 °C, and for comparison, the known complexes 15 and 16 were screened under the conditions employed herein. For the di-nuclear complexes 1–6 (runs 1–6, Table S2†), in terms of the % conversion, these complexes behave similarly, which does not allow for the observation of any significant structure/activity relationships. Given this, we provide only a brief discussion here and the tabulated data can be found in the ESI (Table S2,† runs 1–13). For 1–6, the highest conversion was observed for 5 (R = *t*Bu, R' = Et: 98.0%) and the lowest for 1 (R = R' = Me: 93.2%). For pairs of complexes where R is constant, the ethyl derivatives were more active than the methyl derivatives and the molecular weights (M_n) were higher; such trends have been noted previously;¹⁵ the opposite trends in activity have also been noted.¹⁶ The spread of molecular weights (M_n) [5.14 – 10.12×10^4] also followed no obvious trend, whilst in all cases, the PDI remained relatively constant [1.22–1.49]. However, in all cases, the performance of the oxy bridged systems was superior to that of the di-nuclear $-\text{CH}_2\text{CH}_2-$ bridged complexes 7 and 15, for which the % conversion was only 25.6% and 38.5%, respectively under the conditions employed herein.

In the case of the tetra-nuclear complexes 11–14 (runs 8–11, Table S2†), the complexes bearing methyl at the *para* position of the phenolic group afforded high conversions of about 99%,

whilst the systems (12 and 14), employing a *para* Cl, gave lower conversions of 80.9 and 94.3%, respectively. This may be attributed to observed solubility issues rather than electronic effects. The polymer molecular weight (M_n) associated with 12 and 14 was also somewhat lower than that observed for the other tetra-nuclear systems. Again, the performance of the related $-\text{CH}_2\text{CH}_2-$ bridged complex, namely 16 was inferior under the conditions employed herein affording a % conversion of 29.1% and a much lower molecular weight (M_n). This enhanced activity is tentatively ascribed to the ability of the oxygen bridge to stabilize the catalytically active species, akin to the situation observed in dimethyleneoxa-bridged calixarene systems during ethylene polymerization.¹⁷ As for the di-nuclear systems, the tetra-nuclear ethylaluminium derivatives (13 and 14) were more active than the methylaluminium counterparts (11 and 12).

In general, the resulting PCL polymer molecular weights were in reasonable agreement with the calculated values, which indicates that there are, in most cases, little in the way of *trans*-esterification reactions occurring. However, in the MALDI-ToF mass spectra, as well as the population of peaks separated by 114.14 mass units (see Fig. S13 and S14†), there was evidence of a second, albeit minor, population which is more pronounced at 25 °C. A plot of average molecular weight (M_n) *versus* conversion (Fig. S15†) exhibited a near linear relationship. In the ¹H NMR spectra of the PCL (Fig. S16 and S17†), signals at around 7.34 and 5.15 ppm ($\text{C}_6\text{H}_5\text{CH}_2-$) and 3.62 ($\text{CH}_2\text{CH}_2\text{OH}$), with an integral ratio 5 : 2 : 2, indicated that the polymer chains are capped by a benzyl group and a hydroxy end group.

ROP of *rac*-lactide. Complex 5 was again used to verify the optimum condition for the ROP of *rac*-lactide (see Table 4). At 50 °C, there was no activity (run 6, Table 4), whilst the activity increased on raising the temperature from 80 to 110 °C. Best conversions at 110 °C were achieved with the ratio 100 : 1 : 1 for *rac*-Lac : Al : BnOH, whilst prolonging the screening time from 6 to 24 h only afforded a slight increase in the % conversion. In all cases, the system was relatively well controlled with polydispersities in the range 1.03–1.41.

Complexes 1–14 (not 8–10) were then screened using the ratio 100 : 1 : 1 (*rac*-LA : cat : BnOH) over 12 h at 110 °C



(Table S2,† runs 14–23). The ROP appeared to be well controlled in terms of PDI with values in the range 1.07–1.38. There was no obvious advantage in the use of di- versus tetra-nuclear systems under the conditions employed. For the di-nuclear systems, the ethylaluminium derivatives were slightly more active than their methylaluminium counterparts and the polymers possessed slightly higher molecular weight (M_n), however this trend was not evident for the tetra-nuclear systems. ^1H NMR spectroscopic investigations were conducted in order to verify the polymer molecular weights and to identify the end groups present. The results were similar (e.g. see Fig. S18†) to the results obtained for the PCL runs, i.e. insertion of a benzyloxy group during polymerization. Again, there was reasonable agreement between observed and calculated molecular weights (M_n), whilst MALDI-ToF spectra (e.g. Fig. S19†) revealed a number of minor populations. To assign the stereochemistry of the PLA polymers, we employed 2D J -resolved ^1H NMR (e.g. see Fig. S20 and S21†) and assigned the peaks by reference to the literature.¹⁸ These systems gave moderately isotactic PLA with P_r values in the range 0.64–0.67.

In conclusion, [2 + 2] Schiff base macrocycles of the type $\{[2-(\text{OH})-5-(\text{R})\text{C}_6\text{H}_2-1,3-(\text{CH}_2)_2][\text{O}(2-\text{C}_6\text{H}_4\text{N})_2]\}_2$ ($\text{R} = \text{Me } \text{L}^1\text{H}_2$, $t\text{Bu } \text{L}^2\text{H}_2$, $\text{Cl } \text{L}^3\text{H}_2$) are readily accessible by reacting 2,6-dicarboxy-4- R -phenol with the diamine 2,2'-oxydianiline, $(2-\text{NH}_2\text{C}_6\text{H}_4)_2\text{O}$. The molecular structures of a number of solvates have been determined. The molecular structures of the various solvates reveal a tendency to form a taco-shaped conformation, the cleft angle ϕ associated with the latter varies greatly with that of $\text{L}^1\text{H}_2\cdot\text{MeCN}$ and $\text{L}^2\text{H}_2\cdot 2\text{toluene}$ being very open at about 89° , whilst the other solvates (MeCN , acetone and ethyl acetate) of L^2H_2 were more closed with cleft angles ϕ in the range $8\text{--}17^\circ$. The solvent is only encapsulated by the macrocycle in $\text{L}^1\text{H}_2\cdot\text{MeCN}$. Ethyl acetate and acetone reside in similar locations *exo* to the macrocycle in a series of three pseudo-isomorphous structures. Furthermore, we have found that the interaction of alkylaluminium reagents can be more complicated than originally thought (from studies of the $-\text{CH}_2\text{CH}_2-$ bridged systems) and a number of unexpected products can be formed. In particular, we have found that for the di-nuclear species, 'trans' as well as the previous 'cis' structures can readily be isolated, as can complexes in which one of the methylaluminium centres is bound in tridentate fashion by the macrocycle. Moreover, species in which there are no alkyl groups at aluminium, but where two macrocycles bind such that the Al centre is near octahedral, are readily formed in the presence of limited organoaluminium reagent. Tetra-nuclear complexes can be accessed which have undergone alkyl transfer ($\times 2$) to one side of the macrocycle by employing excess organoaluminium reagent. These organoaluminium species are capable of the ROP of ϵ -caprolactone and *rac*-lactide and can out-perform the related systems bearing $-\text{CH}_2\text{CH}_2-$ bridged Schiff-base macrocycles under similar conditions. However, there appears to be little benefit in the use of di- versus tetra-nuclear species under the ROP conditions employed herein.

Experimental

General

Methanol was dried over magnesium. Hexane was refluxed over sodium and benzophenone. Toluene was refluxed over sodium. Acetonitrile was refluxed over calcium hydride. IR spectra (nujol mulls, KBr windows) were recorded on a Nicolet Avatar 360 FT IR spectrometer; ^1H NMR and ^{13}C NMR spectra were recorded at room temperature on a Varian VXR 400 S spectrometer at 400 MHz or a Gemini 300 NMR spectrometer or a Bruker Advance DPX-300 spectrometer. The ^1H NMR spectra were calibrated against the residual protio impurity of the deuterated solvent. Elemental analyses were performed by the elemental analysis service at the London Metropolitan University, the Chemistry Department at the University of Hull or at Sichuan University, Chengdu. The precursors 2,6-(CHO)₂-4- R - $\text{C}_6\text{H}_2\text{OH}$ and $(2-\text{NH}_2\text{C}_6\text{H}_4)_2\text{O}$ and 2,2'-ethylenediamine and the complexes **15** and **16** were prepared by the literature methods.^{12,19,20} The Schiff-base ligands were prepared as outlined below, and the respective solvates were crystallized by taking about 100 mg of the macrocycle and dissolving in the appropriate solvent. In the case of acetonitrile and toluene, the solvates crystallized out at ambient temperature, whereas for acetone and ethyl acetate, cooling to -20°C was required. For the organoaluminium complexes, all manipulations were carried out under an atmosphere of dry nitrogen using conventional Schlenk and cannula techniques or in a conventional nitrogen-filled glove box. All solvents were distilled and degassed prior to use.

Synthesis of L^1H_2 . 2,6-Dicarboxy-4-Me-phenol (0.82 g, 5.0 mmol) and $(2-\text{NH}_2\text{C}_6\text{H}_4)_2\text{O}$ (1.00 g, 5.0 mmol) were refluxed in dry methanol (50 ml) for 12 h in the presence of a few drops of acetic acid. On cooling, the solvent was removed *in vacuo*, and the residue was extracted into toluene (30 ml). An orange crystalline sample of L^1H_2 was formed on prolonged standing (2–3 days) at ambient temperature, yield 1.20 g, 74%. Single crystals suitable for X-ray crystallography can be grown from a saturated acetonitrile or toluene solution on prolonged standing (slow evaporation) at room temperature. Anal. calcd for $\text{C}_{42}\text{H}_{32}\text{N}_4\text{O}_4\cdot\text{C}_7\text{H}_8$: C, 78.59; H, 5.38; N, 7.48; Found C, 78.77; H, 5.28; N, 7.15%. IR (cm^{-1}): 3068 (w), 3028 (w), 2864 (w), 1626 (s), 1579 (s), 1480 (s), 1453 (s), 1359 (m), 1314 (w), 1240 (s), 1215 (m), 1195 (m), 1155 (w), 1032 (m), 1008 (m), 854 (m), 837 (m), 786 (m), 745 (s), 700 (w), 653 (w), 603 (w), 538 (w), 511 (w), 454 (m); MS (EI^+) m/z : 657 [M]⁺. ^1H NMR (400 MHz, $\text{DMSO}-d_6$) δ : 14.11 (s, 2H, OH), 8.87 (s, 4H, $-\text{CH}=\text{N}$), 7.54 (s, 4H, Ar- H), 7.12–7.24 (m, 16H, Ar- H), 2.27 (s, 3H, $-\text{CH}_3$), 2.24 (s, 3H, $-\text{CH}_3$). ^{13}C NMR (100 MHz, $\text{DMSO}-d_6$) δ : 20.4, 116.0, 116.6, 117.7, 120.1, 124.2, 127.7, 140.1, 143.6, 149.7, 160.4.

Synthesis of L^2H_2 . As for L^1H_2 , but using 2,6-bicarboxy-4-*tert*-butyl-phenol (1.03 g, 5.0 mmol) and $(2-\text{NH}_2\text{C}_6\text{H}_4)_2\text{O}$ (1.00 g, 5.0 mmol), yield 1.1 g, 60%. Anal Calcd for $\text{C}_{48}\text{H}_{44}\text{N}_4\text{O}_4$ (sample dried *in vacuo* for 12 h): C, 77.81; H, 5.99; N, 7.56; Found: C, 77.35; H, 6.43; N, 7.96%. IR (cm^{-1}): 3063 (w), 2954 (m), 2932 (m), 2864 (w), 1630 (s), 1578 (m), 1484 (m),



1452 (w), 1357 (m), 1316 (w), 1238 (s), 1192 (m), 1158 (m), 1034 (m), 1006 (s), 981 (w), 857 (w), 789 (w), 748 (s), 652 (w), 600 (w), 548 (w), 452 (w). MS (EI⁺) *m/z*: 741[M]⁺. ¹H NMR (400 MHz, DMSO-d₆): δ 14.86 (s, 2H, -OH), 8.81 (s, 4H, -CH=N), 7.25 (s, 4H, Ar-H), 7.06–7.25 (m, 16H, Ar-H), (s, 18H, C(CH₃)₃). ¹³C NMR (100 MHz, DMSO-d₆) δ: 31.7, 34.3, 116.0, 116.8, 118.2, 120.6, 124.2, 125.1, 140.1, 140.3, 143.6, 160.9.

Synthesis of L³H₂. As for L¹H₂, but using 2,6-bicarboxy-4-chloro-phenol (0.92 g, 5.0 mmol) and (2-NH₂C₆H₄)₂O (1.00 g, 5.0 mmol), yield 1.4 g, 80%. C₄₀H₂₆N₄O₄Cl₂ (sample dried *in vacuo* for 12 h): C, 68.87; H, 3.76; N, 8.03. Found: C, 69.26; H, 4.16; N, 8.09%. IR (cm⁻¹): 3063 (w), 2924 (w), 2854 (w), 1627 (s), 1598 (w), 1574 (s), 1540 (m), 1483 (s), 1452 (s), 1369 (w), 1352 (m), 1303 (m), 1238 (s), 1209 (m), 1185 (m), 1155 (w), 1108 (m), 1012 (s), 965 (w), 937 (w), 915 (w), 890 (m), 866 (m), 798 (w), 749 (s), 692 (w), 647 (w), 597 (w), 564 (w), 517 (w), 457 (w), 417 (w). MS(EI⁺) *m/z*: 698[M]⁺. ¹H NMR (400 MHz, DMSO-d₆): δ 14.89 (s, 2H, -OH), 8.84 (s, 4H, -CH=N), 7.58 (s, 4H, Ar-H), 7.22–7.34 (m, 12H, Ar-H), 7.07 (d, *J* = 11.2 Hz, 4H, Ar-H). This compound proved to be too insoluble to obtain meaningful ¹³C NMR spectra, even upon heating in DMSO-d₆.

Synthesis of L²(tosyl)₂. The oxydianiline (1.00 g, 4.99 mmol) was combined with 2,6-bicarboxy-4-*tert*-butyl-phenoxytosylate (1.80 g, 4.99 mmol) in ethanol (30 ml) and the system was refluxed for 12 h. The volatiles were removed *in vacuo*, and the residue was extracted in acetonitrile (30 ml). Prolonged standing at ambient temperature afforded orange crystals of L²(tosyl)₂ (1.86 g, 71%). C₆₂H₅₆N₄O₈S₂ (sample dried *in vacuo* for 12 h): C, 70.97; H, 5.38; N, 5.34. Found: C, 70.56; H, 5.16; N, 5.09%. IR (cm⁻¹): 3624 (w), 1927 (w), 1770 (w), 1721 (s), 1620 (s), 1340 (s), 1302 (s), 1261 (s), 1154 (s), 1093 (s), 981 (m), 926 (m), 907 (m), 888 (s), 855 (s), 801 (s), 721 (s), 623 (s), 542 (s), 510 (w), 486 (m). MS (ESI) *m/z*: 895 [MH⁺ - tosyl].

Synthesis of {(Me₂Al)[2-(O)-5-(Me)C₆H₂-1,3-(CH)₂][O(2-C₆H₄)₂N₂]}₂ (1). To the ligand [2,2'-O(C₆H₄N)₂-2,6-(4-MeC₆H₃OH)]₂ (0.50 g, 0.76 mmol) in hexane was added two equivalents of AlMe₃ (0.95 ml, 1.52 mmol), and the system was refluxed for 12 h. The resulting solid was isolated and washed with cold hexane (30 ml) and dried *in vacuo*, to afford **1** as a yellow solid (0.33 g, 56.6%). Elemental analysis calculated for C₄₆H₄₂N₄O₄Al₂: C 71.87, H 5.51, N 7.29%; found: C 71.62, H 5.47, N 7.11%. IR (KBr) cm⁻¹: 3421 (s), 3063 (w), 3014 (w), 2925 (m), 1625 (s), 1592 (s), 1555 (s), 1484 (s), 1451 (s), 1383 (m), 1371 (m), 1336 (w), 1295 (w), 1238 (s), 1216 (s), 1189 (m), 1110 (m), 1039 (m), 990 (m), 932 (w), 863 (m), 833 (m), 789 (m), 750 (s), 711 (m), 686 (m), 606 (w), 546 (w), 457 (w). MS (E.I.) 723.16 [M - 3CH₃]⁺. ¹H NMR (CDCl₃, 400 MHz): δ 8.20 (d, *J* = 2.0 Hz, 2H, C₆H₂), 7.87 (s, 2H, CH=N), 7.56 (d, *J* = 8.0 Hz, 2H, C₆H₂), 7.43 (m, 4H, arylH), 7.31 (d, 4H, arylH), 7.10 (m, H, arylH), 6.99 (d, *J* = 8.4 Hz, 2H, arylH), 6.35 (s, 2H, CH=N), 2.20 (s, 6H, CH₃), -0.74 (s, 6H, Al-CH₃), -0.75 (s, 6H, Al-CH₃).

Synthesis of {(Me₂Al)[2-(O)-5-(*t*Bu)C₆H₂-1,3-(CH)₂][O(2-C₆H₄)₂N₂]}₂ (2). As for **1**, but using [2,2'-O(C₆H₄N)₂-2,6-(4-*t*-BuC₆H₃OH)]₂ (0.50 g, 0.68 mmol) and AlMe₃ (0.84 ml, 1.35 mmol) affording **2** as a yellow solid. Yield: 0.32 g, 55.2%. Elemental analysis calculated for C₅₂H₅₄N₄O₄Al₂: C 73.23,

H 6.38, N 6.57%; found: C 72.97, H 5.96, N 6.95%. IR (cm⁻¹): 3434 (s), 3069 (w), 2958 (m), 2927 (m), 2868 (w), 1623 (s), 1596 (s), 1582 (s), 1545 (s), 1484 (s), 1449 (s), 1391 (w), 1375 (m), 1364 (m), 1328 (w), 1304 (w), 1275 (m), 1242 (s), 1226 (s), 1182 (s), 1111 (m), 1040 (w), 1016 (w), 997 (w), 978 (w), 959 (w), 933 (w), 890 (w), 874 (w), 874 (w), 858 (w), 839 (w), 820 (w), 792 (m), 773 (s), 749 (w), 713 (m), 680 (m), 662 (m), 601 (w), 550 (w). MS (E.I.): 853.5 [M]⁺. ¹H NMR (CDCl₃, 400 MHz) δ 8.35 (d, *J* = 2.0 Hz, 2H, C₆H₂), 8.02 (s, 2H, CH=N), 7.62 (s, 2H, CH=N), 7.50 (d, 2H, *J* = 8.4 Hz, arylH), 7.41–7.46 (m, 2H, arylH), 7.26–7.30 (t, 4H, arylH), 7.11–7.16 (m, 2H, arylH), 7.04–7.08 (m, arylH), 6.99 (dd, 2H, *J*₁ = 7.6 Hz, *J*₂ = 1.6 Hz, arylH), 6.92 (dd, 2H, *J*₁ = 8.0 Hz, *J*₂ = 1.2 Hz, arylH), 6.70–6.71 (d, 2H, *J* = 2.8 Hz, C₆H₂), 1.26 (s, 18H, (CH₃)₃), -0.83 (s, 6H, Al-CH₃), -0.84 (s, 6H, Al-CH₃).

Synthesis of {(Me₂Al)[2-(O)-5-(Cl)C₆H₂-1,3-(CH)₂][O(2-C₆H₄)₂N₂]}₂ (3). As for **1**, but using [2,2'-O(C₆H₄N)₂-2,6-(4-Cl-C₆H₃OH)]₂ (0.50 g, 0.72 mmol) and AlMe₃ (0.90 ml, 1.43 mmol) affording **3** as a yellow solid. Yield: 0.36 g, 61.8%. Elemental analysis calculated for C₄₄H₃₆N₄O₄Cl₂Al₂: C 65.28, H 4.48, N 6.92%; found: C 64.81, H 4.50, N 6.95%. IR (cm⁻¹): 3409 (s), 3064 (m), 2962 (m), 2930 (m), 2872 (m), 1610 (s), 1577 (s), 1550 (m), 1502 (s), 1487 (s), 1449 (s), 1374 (m), 1328 (m), 1261 (s), 1235 (s), 1212 (s), 1158 (s), 1105 (m), 1045 (m), 930 (w), 866 (w), 800 (w), 744 (s), 694 (w), 620 (w), 465 (w). MS (E. I.): 831.0 [M + Na]⁺. ¹H NMR (CDCl₃, 400 MHz): δ 8.34 (d, *J* = 2.8 Hz, 2H, C₆H₂), 7.97 (s, 2H, CH=N), 6.97–7.58 (m, 18H, arylH), 6.59 (d, *J* = 2.8, 2H, CH=N), -0.67 (s, 6H, Al-CH₃), -0.73 (s, 6H, Al-CH₃).

Synthesis of {(Et₂Al)[2-(O)-5-(Me)C₆H₂-1,3-(CH)₂][O(2-C₆H₄)₂N₂]}₂ (4). To the ligand [2,2'-O(C₆H₄N)₂-2,6-(4-MeC₆H₃OH)]₂ (0.50 g, 0.76 mmol) in hexane was added two equivalents of AlEt₃ (0.76 ml, 1.52 mmol) affording **4** as a yellow solid (yield 0.39 g, 62.3%). Elemental analysis calculated for C₅₀H₅₀N₄O₄Al₂: C 72.80, H 6.11, N 6.79%; found: C 72.45, H 5.98, N 6.95%. IR (KBr) cm⁻¹: 3434 (s), 3067 (w), 2925 (w), 2891 (w), 2855 (w), 1793 (w), 1734 (w), 1625 (s), 1595 (s), 1552 (s), 1485 (s), 1452 (s), 1383 (s), 1333 (w), 1304 (w), 1273 (m), 1233 (s), 1217 (m), 1192 (m), 1163 (w), 1111 (m), 1043 (w), 990 (m), 946 (w), 932 (w), 877 (w), 859 (w), 832 (w), 791 (w), 754 (m), 742 (m), 670 (w), 647 (w), 612 (m), 565 (w), 545 (w), 454 (w), 419 (w). MS (E.I.): 849.8 [M + Na]⁺. ¹H NMR (CDCl₃, 400 MHz) δ 8.16 (d, 2H, *J* = 4.8 Hz, C₆H₂), 7.91 (s, 2H, CH=N), 7.57 (d, *J* = 8.0 Hz, 2H, arylH), 7.52 (s, 2H, CH=N), 7.43–7.48 (m, 2H, arylH), 7.34 (m, 4H, arylH), 7.06–7.13 (m, 6H, arylH), 6.39 (dd, *J* = 8.0 Hz, *J* = 1.6 Hz, 2H, arylH), 6.39 (d, 2H, *J* = 2.4 Hz, C₆H₂), 2.19 (s, 6H, CH₃), 0.94 (t, *J* = 8.0 Hz, 6H, Al-CH₂CH₃), 0.74 (t, *J* = 8.4 Hz, 6H, Al-CH₂CH₃), -0.07 to -0.09 (overlapping m, 8H, Al-CH₂CH₃).

Synthesis of {(Et₂Al)[2-(O)-5-(*t*Bu)C₆H₂-1,3-(CH)₂][O(2-C₆H₄)₂N₂]}₂ (5). To the ligand [2,2'-O(C₆H₄N)₂-2,6-(4-*t*-BuC₆H₃OH)]₂ (0.50 g, 0.68 mmol) in hexane was added two equivalents of AlEt₃ (0.72 ml, 1.44 mmol) affording **5** as a yellow solid (yield 0.41 g, 66.4%). Elemental analysis calculated for C₅₆H₆₂N₄O₄Al₂: C 73.99, H 6.87, N 6.16%; found: C 73.51, H 6.68, N 5.83%. IR (KBr) cm⁻¹: 2929 (w), 2858 (w),



1621 (s), 1577 (m), 1545 (s), 1484 (s), 1447 (s), 1381 (w), 1320 (w), 1300 (w), 1244 (m), 1214 (m), 1182 (m), 1157 (m), 1110 (m), 1030 (m), 1014 (w), 983 (w), 937 (w), 870 (w), 856 (w), 838 (w), 810 (w), 792 (w), 752 (s), 705 (w), 668 (w), 649 (w), 602 (w), 476 (w). MS (E.I.): 863.55 [M]⁺. ¹H NMR (CDCl₃, 400 MHz): δ 8.29 (d, *J* = 2.4 Hz, 2H, C₆H₂), 8.10 (s, 2H, CH=N), 7.73 (s, 2H, CH=N), 6.97–7.46 (m, 16H, arylH), 6.06 (d, *J* = 2.8 Hz, C₆H₂), 0.94 (t, *J* = 8.0 Hz, 6H, Al-CH₂CH₃), 0.63 (t, *J* = 8.0 Hz, 6H, Al-CH₂CH₃), -0.06 to -0.22 (overlapping m, 8H, Al-CH₂CH₃).

Synthesis of {(Et₂Al)[2-(O)-5-(Cl)C₆H₂-1,3-(CH)₂][O(2-C₆H₄)₂N₂]}₂ (6). To the ligand [2,2'-O(C₆H₄N)₂-2,6-(4-Cl-C₆H₃OH)]₂ (0.50 g, 0.72 mmol) in hexane was added two equivalents of AlEt₃ (0.72 ml, 1.44 mmol) affording **6** as a yellow solid. Yield: 0.42 g, 67.5%. Elemental analysis calculated for C₄₈H₄₄N₄O₄Cl₂Al₂: C 66.59, H 5.12, N 6.47%; found: C 66.15, H 5.35, N 6.21%. IR (KBr): cm⁻¹ 2929 (w), 2858 (w), 1621 (s), 1577 (m), 1545 (s), 1484 (s), 1447 (s), 1381 (w), 1320 (w), 1300 (w), 1244 (m), 1214 (m), 1182 (m), 1157 (m), 1110 (m), 1030 (m), 1014 (w), 983 (w), 937 (w), 870 (w), 856 (w), 838 (w), 810 (w), 792 (w), 752 (s), 705 (w), 668 (w), 649 (w), 602 (w), 476 (w). MS (E.I.): 863.55 [M]⁺. ¹H NMR (CDCl₃, 400 MHz): δ 8.29 (d, *J* = 2.4 Hz, 2H, C₆H₂), 8.02 (s, 2H, CH=N), 7.02–7.73 (m, 18H, arylH), 6.06 (d, *J* = 4.2 Hz, C₆H₂), 0.94 (t, *J* = 8.0 Hz, 6H, Al-CH₂CH₃), 0.73 (t, *J* = 8.0 Hz, 6H, Al-CH₂CH₃), -0.05 to -0.11 (overlapping m, 8H, Al-CH₂CH₃).

Synthesis of {(Me₂Al)(MeAl)[2-(O)-5-(tBu)C₆H₂-1,3-(CH)₂][(CH₂CH₂)(2-C₆H₄)₂N₂]}₂·2¹/₄MeCN (7·2¹/₄MeCN). To the ligand [2,2'-CH₂CH₂(C₆H₄N)₂-2,6-(4-tBuC₆H₃OH)]₂ (0.50 g, 0.65 mmol) in toluene was added two equivalents of AlMe₃ (0.69 ml, 2 M solution in toluene, 1.38 mmol), and the system was refluxed for 12 h. Following removal of volatiles *in vacuo*, the residue was extracted in MeCN (30 cm³), and on prolonged standing at room temperature afforded small orange crystals of 7·2¹/₄MeCN. Yield: 0.13 g, 24%. Elemental analysis calculated for C_{59.5}H_{66.75}N_{6.25}O₂Al₂: C 74.80, H 7.04, N 9.16%; found: C 74.59, H 6.84, N 9.08%. IR (KBr) cm⁻¹: 3646 (w), 1650 (w), 1590 (m), 1261 (s), 1234 (m), 1199 (m), 1149 (m), 1107 (bs), 1005 (s), 922 (w), 904 (w), 881 (m), 797 (s), 753 (m), 635 (m).

Synthesis of {(Et₂Al)[2-(O)-5-(Me)C₆H₂-1,3-(CH)₂][(CH₂CH₂)(2-C₆H₄)₂N₂]}₂ (8). To the ligand [2,2'-CH₂CH₂(C₆H₄N)₂-2,6-(4-MeC₆H₃OH)]₂ (0.50 g, 0.74 mmol) in toluene was added two equivalents of AlEt₃ (0.73 ml, 1.47 mmol), and the system was refluxed for 12 h. Following removal of volatiles *in vacuo*, the residue was extracted in MeCN (30 cm³), and on prolonged standing at room temperature afforded small yellow crystals of **8**. Yield: 0.35 g, 55.8%. Elemental analysis calculated for C₅₄H₅₈N₄O₂Al₂: C 76.39, H 6.88, N 6.60%; found: C 76.59, H 6.44, N 7.08%. IR (KBr) cm⁻¹: 1626 (m), 1592 (w), 1556 (m), 1339 (w), 1261 (s), 1240 (w), 1210 (w), 1191 (w), 1177 (w), 1157 (w), 1094 (s), 1019 (s), 947 (w), 918 (w), 870 (w), 800 (s), 769 (m), 749 (m), 740 (w), 727 (m), 694 (w), 671 (w), 646 (w), 628 (w). MS (MALDI-ToF): 764 (M⁺ - 2Et - Al). ¹H NMR (CDCl₃, 400 MHz): δ 8.24 (s, 2H, CH=N), 8.17 (d, 2H, *J* = 2.0 Hz, C₆H₂), 7.60 (d, *J* = 7.60 Hz, 2H, arylH), 7.40 (t, 2H, *J* = 7.2 Hz, arylH), 7.26 (t, 4H, *J* = 6.0 Hz, arylH), 6.99 (d, 2H, *J* = 5.6 Hz, arylH),

6.90 (t, 2H, *J* = 7.2 Hz, arylH), 6.81 (d, 2H, *J* = 7.6 Hz, arylH), 6.68 (d, 2H, *J* = 2.4 Hz, C₆H₂), 6.62 (d, 2H, *J* = 6.8 Hz, arylH), 6.42 (s, 2H, CH=N), 3.81 (dt, *J*₁ = 12.8 Hz, *J*₂ = 4.0 Hz, 2H, CH₂), 3.69 (td, *J*₁ = 13.2 Hz, *J*₂ = 4.0 Hz, 2H, CH₂), 3.01 (dt, *J*₁ = 14.0 Hz, *J*₂ = 4.8 Hz, 2H, CH₂), 2.68 (td, *J*₁ = 12.8 Hz, *J*₂ = 4.4 Hz, 2H, CH₂), 2.41 (s, 6H, CH₃), 0.94 (t, 6H, *J* = 8.4 Hz, Al-CH₂CH₃), 0.72 (t, 6H, *J* = 8.0 Hz, Al-CH₂CH₃), 0.05 (m, 4H, Al-CH₂), 0.32 (m, 4H, Al-CH₂).

Synthesis of [Al(L³)(L³H)]·4toluene (9·4toluene). To the ligand [2,2'-O(C₆H₄N)₂-2,6-(4-ClC₆H₃OH)]₂ (0.50 g, 0.72 mmol) in hexane (30 ml) was added AlEt₃ (0.20 ml, 1.9 M, 0.38 mmol), and the system was refluxed for 12 h. Following removal of volatiles *in vacuo*, the residue was extracted in MeCN (30 cm³), and on prolonged standing at room temperature afforded small yellow/orange crystals of **9**·4toluene. Yield: 0.24 g, 48%. Elemental analysis calculated for C₈₀H₅₀N₈O₈Cl₄Al: C 67.67, H 3.55, N 7.89%; found (sample dried *in vacuo* for 12 h): C 66.59*, H 3.74, N 7.38%. *Despite repeated analyses, this was the best result for % C. IR (KBr) cm⁻¹: 2360 (m), 2341 (m), 1716 (w), 1616 (w), 1576 (w), 1540 (m), 1301 (m), 1260 (s), 1208 (w), 1093 (s), 1020 (s), 867 (m), 800 (s), 722 (m), 688 (w), 467 (w). MS (positive ion nanospray): 1278.3 (M⁺ - 4Cl); (MALDI-ToF, no matrix): 722.5 (M⁺ - L³H₂). ¹H NMR (CDCl₃, 400 MHz): δ 8.90 (bs, 4H, CH=N), 8.50 (s, 2H, CH=N), 8.32 (s, 2H, CH=N), 7.61 (s, 4H, Ar-H), 7.25–7.12 (m, 28H, Ar-H), 7.02 (overlapping m, 10H, Ar-H).

Synthesis of [Al(L⁵)(L⁵H)]·5MeCN (10·5MeCN). To the ligand [2,2'-CH₂CH₂(C₆H₄N)₂-2,6-(4-tBuC₆H₃OH)]₂ (0.50 g, 0.65 mmol) in hexane (30 ml) was added AlEt₃ (0.20 ml, 1.9 M, 0.38 mmol), and the system was refluxed for 12 h. Following removal of volatiles *in vacuo*, the residue was extracted in MeCN (30 cm³), and on prolonged standing at room temperature afforded small yellow crystals of **10**·5MeCN. Yield: 0.19 g, 37%. Elemental analysis calculated for C₁₁₂H₁₁₃N₁₂O₄Al: C 78.30, H 6.63, N 9.78%; found (sample dried *in vacuo* for 12 h): C 77.89, H 6.44, N 9.48%. IR (KBr) cm⁻¹: 1630 (s), 1588 (m), 1573 (s), 1307 (m), 1262 (s), 1206 (m), 1155 (m), 1089 (s), 1034 (s), 1018 (s), 880 (w), 861 (w), 801 (m), 770 (w), 753 (m), 722 (s), 647 (w), 636 (w), 613 (w), 596 (w), 566 (w), 530 (w), 506 (w), 464 (w). MS (MALDI-ToF, no matrix): 790 (M⁺ - LH). ¹H NMR (CDCl₃, 400 MHz): δ 8.83 (bs, 2H, CH=N), 8.71 (bs, 2H, CH=N), 8.35 (bs, 4H, CH=N), 8.29 (m, 2H, arylH), 7.91–6.18 (overlapping m, 32 H, arylH), 5.88 (d, 2H, arylH), 5.86 (d, 2H, *J* = 18.0 Hz, arylH), 5.62 (d, 2H, *J* = 14.4 Hz, arylH), 5.34 (bm, 2H, CH₂), 4.56 (bm, 2H, CH₂), 3.86 (bm, 2H, CH₂), 3.74 (bm, 2H, CH₂), 3.30 (bm, 2H, CH₂), 3.13 (overlapping m, 2H, CH₂), 3.07 (bm, 2H, CH₂), 2.91 (bm, 2H, CH₂), 2.44 (s, 3H, MeCN), 2.01 (s, 3H, MeCN), 0.92 (s, 6H, MeCN), 1.56 (s, 9H, C(CH₃)₃), 1.41 (s, 9H, C(CH₃)₃), 1.29 (s, 9H, C(CH₃)₃), 1.19 (s, 9H, C(CH₃)₃).

Synthesis of {(Me₂Al)₂[2-(O)-5-(tBu)C₆H₂-1-(CH)-3-C(Me)H]-[(O)(2-(N)-2'-C₆H₄N)₂]}₂·1.75toluene·1.25hexane (11·1.75toluene·1.25hexane). As for **1**, but using [2,2'-O(C₆H₄N)₂-2,6-(4-t-BuC₆H₃OH)]₂ (0.50 g, 0.68 mmol) and AlMe₃ (1.7 ml, 2.70 mmol) and then recrystallisation from a saturated hexane/toluene (50:50) solution at 0 °C afforded **11**·1.75toluene·1.25hexane as a red crystalline solid on prolonged standing



at 0 °C (1–2 days). Yield 0.25 g, 36.9%. Elemental analysis calculated for $C_{58}H_{72}N_4O_4Al_4$: C 69.87, H 7.28, N 5.62%; found (sample dried *in vacuo* for 12 h): C 69.52, H 6.93, N 5.22%. IR (cm^{-1}): 3413 (s), 3064 (m), 2929 (m), 2857 (m), 1624 (s), 1608 (s), 1551 (m), 1508 (s), 1486 (s), 1456 (s), 1377 (w), 1329 (m), 1261 (s), 1233 (m), 1192 (m), 1157 (w), 1101 (s), 1024 (s), 863 (m), 801 (w), 741 (m), 660 (w). MS (E.I.): 1017.43 $[M + Na]^+$. 1H NMR ($CDCl_3$, 400 MHz): δ 8.29 (d, $J = 2.4$ Hz, 2H, C_6H_2), 8.02 (s, 2H, $CH=N$), 7.02–7.73 (m, 16H, arylH), 6.06 (d, 2H, $J = 4.2$ Hz, C_6H_2), 4.55 (m, 1H, $CHCH_3$), 4.28 (m, 1H, $CHCH_3$), 1.66 (d, 3H, CH_3CH), 1.53 (d, 3H, CH_3CH), 1.25 (s, 9H, $C(CH_3)_3$), 0.89 (s, 9H, $C(CH_3)_3$), -0.52 (2 \times s, 6H, Al- CH_3), -0.77 (s, 3H, Al- CH_3), -0.87 (s, 3H, Al- CH_3), -0.89 (s, 3H, Al- CH_3), -1.14 (s, 3H, Al- CH_3), -1.37 (s, 3H, Al- CH_3), -1.39 (s, 3H, Al- CH_3).

Synthesis of $\{(Me_2Al)_2[2-(O)-5-(Cl)C_6H_2-1-(CH)-3-C(Me)H]-(O)-(2-(N)-2'-C_6H_4N)_2]\}_2$ (12). As for **9**, but using $[2,2'-O(C_6H_4N)_2-2,6-(4-Cl-C_6H_3OH)]_2$ (0.50 g, 0.72 mmol) and $AlMe_3$ (1.8 ml, 2.87 mmol), affording **12** as a red crystalline solid on prolonged standing at ambient temperature (1–2 days). Yield: 0.30 g, 43.8%. Elemental analysis calculated for $C_{50}H_{54}N_4O_4Cl_2Al_4$: C 62.96, H 5.71, N 5.87%; found: C 62.39, H 5.47, N 5.96%. IR (cm^{-1}): 3434 (s), 3061 (w), 2928 (w), 1619 (s), 1597 (m), 1576 (m), 1543 (s), 1447 (s), 1384 (m), 1321 (m), 1301 (w), 1246 (s), 1212 (s), 1183 (m), 1160 (w), 1104 (s), 1031 (s), 940 (w), 868 (w), 839 (w), 810 (m), 753 (m), 709 (w), 699 (m), 685 (w), 636 (w), 579 (w), 447 (w), 529 (w), 476 (w). MS (E.I.): 917.18 $[M - Cl]^+$. 1H NMR ($CDCl_3$, 400 MHz): δ 8.07 (s, 2H, $CH=N$), 7.43 (td, 2H, $J_1 = 8.4$ Hz, $J_2 = 1.6$ Hz, arylH), 7.36 (m, 2H, arylH), 7.32 (dd, 2H, $J_1 = 7.2$ Hz, $J_2 = 1.6$ Hz, arylH), 7.27 (d, 2H, $J = 2.8$ Hz, C_6H_2), 7.18 (m, 2H, arylH), 7.08 (td, 2H, $J_1 = 8.4$ Hz, $J_2 = 1.6$ Hz, arylH), 6.99 (d, 2H, $J = 7.6$ Hz, arylH), 6.71 (d, 2H, $J = 2.4$ Hz, C_6H_2), 6.52 (m, 4H, arylH), 4.47 (q, 2H, $J = 7.2$ Hz, $CHCH_3$), 1.59 (d, 6H, $J = 7.2$ Hz, $CHCH_3$), -0.49 (s, 6H, Al- CH_3), -0.73 (s, 6H, Al- CH_3), -0.83 (s, 6H, Al- CH_3), -1.01 (s, 6H, Al- CH_3).

Synthesis of $\{(Et_2Al)_2[2-(O)-5-(Me)C_6H_2-1-(CH)-3-C(Et)H]-(O)-(2-(N)-2'-C_6H_4N)_2]\}_2$ (13). As for **9**, but using $[2,2'-O(C_6H_4N)_2-2,6-(4-MeC_6H_3OH)]_2$ (0.50 g, 0.76 mmol) $AlEt_3$ (1.5 ml, 2 M, 3.04 mmol), affording **13** as a purple solid on prolonged standing at ambient temperature (1–2 days). Yield: 0.24 g, 30%. Elemental analysis calculated for $C_{62}H_{80}N_4O_4Al_4 \cdot 4$ toluene: C 76.03, H 7.94, N 3.94%; found: C 76.47, H 7.61, N 4.09%. IR (cm^{-1}): 3413 (s), 3064 (m), 2929 (m), 2857 (m), 1624 (s), 1608 (s), 1551 (m), 1508 (s), 1486 (s), 1456 (s), 1377 (w), 1329 (m), 1261 (s), 1233 (m), 1192 (m), 1157 (w), 1101 (s), 1024 (s), 863 (m), 801 (w), 741 (m), 660 (w). MS (E.I.): 1421.8 $[M + 4$ toluene] $^+$, 995.4 $[M - 2Et]^+$, 966.4 $[M - 3Et]^+$, 937.4 $[M - 4Et]^+$. 1H NMR ($CDCl_3$, 400 MHz): δ 7.99 (s, 2H, arylH), 7.49 (dd, 2H, $J_1 = 7.6$ Hz, $J_2 = 1.2$ Hz, arylH), 7.46 (dd, 2H, $J = 1.2$ Hz, C_6H_2), 7.35 (td, 2H, $J_1 = 7.6$, $J_2 = 2.0$ Hz, arylH), 7.16 (td, 2H, $J_1 = 7.6$ Hz, $J_2 = 2.0$ Hz, arylH), 7.07 (dd, 2H, $J_1 = 8.0$ Hz, $J_2 = 2.0$ Hz, arylH), 7.02–7.05 (m, 4H, arylH), 6.96 (dd, 2H, $J_1 = 8.0$ Hz, $J_2 = 2.0$ Hz, arylH), 6.93 (dd, 2H, $J_1 = 8.0$ Hz, $J_2 = 2.0$ Hz, arylH), 6.85 (td, 2H, $J_1 = 8.4$ Hz, $J_2 = 2.0$ Hz, arylH), 6.68 (td, 2H, $J_1 = 8.4$ Hz, $J_2 = 2.0$ Hz, arylH), 6.62 (td, 2H, $J_1 = 8.4$ Hz, $J_2 = 1.2$ Hz, arylH), 6.75 (dd, 2H, $J_1 = 8.4$ Hz, $J_2 = 1.2$ Hz, arylH),

6.61 (dd, 2H, $J_1 = 8.4$ Hz, $J_2 = 1.2$ Hz, arylH), 6.53 (m, 4H, arylH), 6.20 (td, 2H, $J_1 = 8.4$ Hz, $J_2 = 1.2$ Hz, arylH), 6.14 (d, 2H, $J = 13.2$ Hz, C_6H_2) (the aromatic region is a combination of 4 toluene + **13**), 5.61 (s, 2H, $CH=N$), 4.55 (m, 2H, NCH_2Et), 2.26 (m, 2H, $CHCH_2CH_3$), 2.17 (m, 2H, CH_2CH_3), 1.91 (s, 6H, CH_3 toluene), 1.84 (s, 6H, CH_3 toluene), 1.63 (m, 6H, CH_3), 1.49 (m, 2H, $AlCH_2CH_3$), 1.42 (m, 2H, $AlCH_2CH_3$), 0.94 (overlapping m, 12H, $CHCH_2CH_3 + Al-CH_2CH_3$), 0.78 (t, $J = 8.4$ Hz, 6H, $Al-CH_2CH_3$), 0.53 (t, $J = 7.2$ Hz, 6H, $Al-CH_2CH_3$), 0.42 (t, $J = 8.2$ Hz, 6H, $Al-CH_2CH_3$), -0.05 (m, 4H, $Al-CH_2CH_3$), -0.26 (m, 4H, $Al-CH_2CH_3$), -1.21 (m, 2H, $Al-CH_2CH_3$) and -1.50 (m, 2H, $Al-CH_2CH_3$).

Synthesis of $\{(Et_2Al)_2[2-(O)-5-(Cl)C_6H_2-1-(CH)-3-C(Et)H]-(O)-(2-(N)-2'-C_6H_4N)_2]\}_2$ (14). As for **9**, but using $[2,2'-O(C_6H_4N)_2-2,6-(4-Cl-C_6H_3OH)]_2$ (0.50 g, 0.72 mmol) and $AlEt_3$ (1.44 ml, 2 M, 2.88 mmol) affording **14** as a purple solid on prolonged standing at ambient temperature (1–2 days). Yield 0.43 g, 54%. Elemental analysis calculated for $C_{60}H_{74}N_4O_4Cl_2Al_4$: C 65.87, H 6.82, N 5.12%; found: C 65.47, H 6.63, N 4.94%. MS (E.I.): 1116.4 $[M + Na]^+$. IR (cm^{-1}): 1618 (w), 1551 (w), 1304 (m), 1261 (s), 1208 (w), 1153 (w), 1096 (s), 1020 (s), 918 (w), 890 (w), 801 (s), 722 (m), 660 (w), 619 (w), 467 (w). 1H NMR ($CDCl_3$, 400 MHz) δ 8.54 (s, 2H, C_6H_2), 7.63 (dd, 2H, $J_1 = 7.2$ Hz, $J_2 = 1.6$ Hz, arylH), 7.60 (s, 2H, arylH), 7.49 (td, 2H, $J_1 = 7.6$ Hz, $J_2 = 1.6$ Hz, arylH), 7.41 (s, 2H, arylH), 7.33 (dd, 2H, $J_1 = 7.6$ Hz, $J_2 = 1.6$ Hz, arylH), 7.26–7.31 (m, 4H, arylH), 7.22 (td, 2H, $J_1 = 9.2$ Hz, $J_2 = 1.6$ Hz, arylH), 7.16 (m, 2H, $J_1 = 9.2$ Hz, $J_2 = 1.6$ Hz, arylH), 7.09 (dd, 2H, $J_1 = 8.0$ Hz, $J_2 = 1.6$ Hz, arylH), 7.00 (td, 2H, $J_1 = 8.4$, $J_2 = 1.2$ Hz, arylH), 6.95 (2 \times s, 2H, $J = 2.8$ Hz, arylH), 6.82 (td, 2H, $J_1 = 8.4$, $J_2 = 1.2$ Hz, arylH), 6.75 (dd, 2H, $J_1 = 8.4$ Hz, $J_2 = 1.2$ Hz, arylH), 6.61 (dd, 2H, $J_1 = 8.4$, $J_2 = 1.2$ Hz, arylH), 6.33 (dd, 2H, $J_1 = 8.8$ Hz, $J_2 = 1.2$ Hz, arylH) (these peaks are a combination of 2.8toluene plus **14**), 6.14 (s, 2H, $CH=N$), 4.60 (m, 2H, $J_1 = 9.6$, $J_2 = 1.4$ Hz, CH_2Et), 2.36 (m, 2H, $CHCH_2CH_3$), 2.20 (m, 2H, $CHCH_2CH_3$), 2.10 (s, 8.4H, CH_3 of 2.8toluene), 1.77 (m, 2H, $Al-CH_2CH_3$), 1.65 (m, 2H, $Al-CH_2CH_3$), 1.02 (overlapping m, $J = 8.0$ Hz, 12H, $CHCH_2CH_3 + Al-CH_2CH_3$), 0.86 (t, $J = 7.2$ Hz, 6H, $Al-CH_2CH_3$), 0.74 (t, $J = 8.2$ Hz, 6H, $Al-CH_2CH_3$), 0.52 (t, $J = 8.2$ Hz, 6H, $Al-CH_2CH_3$), 0.04 (m, 4H, $Al-CH_2CH_3$), -0.14 (m, 4H, $Al-CH_2CH_3$), -1.13 (m, 2H, $Al-CH_2CH_3$), -1.41 (m, 2H, $Al-CH_2CH_3$).

ROP procedure

ϵ -Caprolactone. Typical polymerisation procedures in the presence of one equivalent of benzyl alcohol (Table 4, run 1) are as follows. A toluene solution of **2** (0.010 mmol, in 1.0 mL toluene) and BnOH (0.010 mmol) were added into a Schlenk tube in the glove-box at room temperature. The solution was stirred for 2 min, and then ϵ -caprolactone (2.5 mmol) along with 1.5 mL toluene was added to the solution. The reaction mixture was then placed into an oil bath pre-heated to the required temperature, and the solution was stirred for the prescribed time. The polymerisation mixture was then quenched by addition of an excess of glacial acetic acid (0.2 mL) into the solution, and the resultant solution was then poured into



Table 5 Crystallographic data for L¹H₂·MeCN, L²H₂·MeCN, L²H₂·*n*(MeCOOEt), *n* = 1 and 2, L²H₂·2(Me₂CO), L²H₂·2(PhMe) and L²(tosyl)₂

Compound	L ¹ H ₂ ·MeCN	L ² H ₂ ·MeCN	L ² H ₂ ·MeCOOEt	L ² H ₂ ·2(MeCOOEt)	L ² H ₂ ·2(Me ₂ CO)	L ² H ₂ ·2(PhMe)	L ² (tosyl) ₂
Formula	C ₄₂ H ₃₂ N ₄ O ₄ ·C ₂ H ₃ N	C ₄₈ H ₄₄ N ₄ O ₄ ·C ₂ H ₃ N	C ₄₈ H ₄₄ N ₄ O ₄ ·C ₄ H ₈ O ₂	C ₄₈ H ₄₄ N ₄ O ₄ ·2(C ₄ H ₈ O ₂)	C ₄₈ H ₄₄ N ₄ O ₄ ·2(C ₃ H ₆ O)	C ₄₈ H ₄₄ N ₄ O ₄ ·2(C ₇ H ₈)	C ₆₂ H ₅₆ N ₄ O ₈ S ₂
Formula weight	697.77	781.92	828.97	917.08	857.02	925.14	1049.23
Crystal system	Triclinic	Triclinic	Monoclinic	Monoclinic	Monoclinic	Monoclinic	Monoclinic
Space group	<i>P</i> $\bar{1}$	<i>P</i> $\bar{1}$	<i>C2/c</i>	<i>C2/c</i>	<i>C2/c</i>	<i>P2₁/n</i>	<i>P2₁/n</i>
Unit cell dimensions							
<i>a</i> (Å)	11.0841(6)	15.1737(5)	24.8335(10)	24.9034(15)	24.5582(10)	13.8127(5)	13.201(3)
<i>b</i> (Å)	12.2117(6)	15.3473(6)	11.2046(4)	11.5371(6)	12.1677(7)	16.8060(6)	13.348(3)
<i>c</i> (Å)	13.8841(7)	19.2180(7)	15.9714(11)	16.9261(12)	16.0892(7)	22.5196(9)	14.966(3)
α (°)	86.1299(8)	98.169(13)	90	90	90	90	90
β (°)	74.9778(8)	109.862(3)	101.497(6)	96.003(6)	98.942(4)	105.428(4)	94.913(3)
γ (°)	89.6361(8)	91.656(3)	90	90	90	90	90
<i>V</i> (Å ³)	1810.81(16)	4152.1(3)	4354.9(4)	4836.4(5)	4749.3(4)	5039.2(3)	2627.4(10)
<i>Z</i>	2	4	4	4	4	4	2
Temperature (K)	150(2)	140(2)	120.0(2)	120.0(2)	293(2)	130.0(1)	150(2)
Wavelength (Å)	0.71073	0.71073	0.71073	0.71073	0.71073	0.71073	0.71073
Calculated density (g cm ⁻³)	1.280	1.251	1.264	1.259	1.199	1.219	1.326
Absorption coefficient (mm ⁻¹)	0.08	0.08	0.083	0.084	0.078	0.076	0.164
Transmission factors (min./max.)	0.947, 0.979	0.942, 1.062	0.784, 1.000	0.799, 1.000	0.952, 1.000	0.709, 1.000	0.960, 0.985
Crystal size (mm ³)	0.66 × 0.45 × 0.25	0.38 × 0.29 × 0.10	0.49 × 0.40 × 0.38	0.48 × 0.42 × 0.27	0.20 × 0.20 × 0.30	0.50 × 0.40 × 0.30	0.25 × 0.18 × 0.09
θ (max) (°)	29.0	22.5	27.5	25.0	25.0	25.0	25.0
Reflections measured	16 012	33 814	12 474	12 476	9158	27 782	19214
Unique reflections	8329	10 758	4880	4267	4173	8856	4626
<i>R</i> _{int}	0.013	0.086	0.031	0.032	0.018	0.055	0.051
Reflections with $F^2 > 2\sigma(F^2)$	6933	5230	3517	3777	3045	6118	3019
Number of parameters	487	1093	303	365	323	654	360
<i>R</i> ₁ [$F^2 > 2\sigma(F^2)$]	0.050	0.043	0.049	0.117	0.047	0.059	0.051
w <i>R</i> ₂ (all data)	0.141	0.083	0.130	0.253	0.133	0.154	0.163
GOOF, <i>S</i>	1.023	0.788	1.058	1.222	1.049	1.048	1.070
Largest difference peak and hole (e Å ⁻³)	1.30 and -0.53	0.32 and -0.28	0.25 and -0.31	0.37 and -0.39	0.14 and -0.16	0.68 and -0.36	0.33 and -0.54



methanol (200 mL). The resultant polymer was then collected on filter paper and was dried *in vacuo*.

rac-Lactide. 5 mL of dry toluene were transferred into a Schlenk tube containing the desired amount of catalyst. The solution was stirred and maintained at the polymerisation temperature with the aid of an oil bath. Benzyl alcohol was then added from a 0.6 M solution in toluene. After an additional five minutes, the polymerisation was started by the addition of 1.0 mL of *rac*-lactide.

Experimental crystallography

Diffraction data for L^1H_2 -MeCN and $L^2(\text{tosyl})_2$ were measured on Bruker SMART 1000 CCD and APEX 2 CCD diffractometers respectively, with Mo-K α radiation, at 150(2) K using 0.3 $^\circ$ ω -scans.²¹ Corrections were made for absorption and for Lorentz and Lp effects.²¹ The structures were solved by direct methods and refined on F^2 by full-matrix-least squares.²²

For the L^2H_2 .solv. samples, diffraction intensities were measured on Oxford Diffraction Xcalibur-3 or New Gemini CCD diffractometers equipped with Mo-K α radiation and graphite monochromator. The data for L^2H_2 ·2(acetone) were recorded at room temperature but the other samples were measured at temperatures between 120 and 140 K. Intensity data were measured by thin-slice ω - and ϕ -scans. Data were processed using the CrysAlis-CCD and -RED²³ programs. The structures were determined by the direct methods routines in

the SHELXS program²² and refined by full-matrix least-squares methods, on F^2 , in SHELXL.²²

For 7·2 $\frac{1}{4}$ MeCN, data collected at Daresbury Laboratory Station 9.8.²¹ The crystal was weakly diffracting, so data were only integrated to $2\theta = 45^\circ$. The *t*Bu group at C89 was modeled as two-fold disordered with a major component of 72.8(9)%, whilst the MeCN containing N12 was refined at half weight. For **8**, data were collected using an Agilent Xcalibur diffractometer with an Eos detector. Single crystal diffraction data for 9·4toluene and 10·5MeCN were collected by the UK National Crystallography Service using a Rigaku FR-E+ diffractometer. This operates with a SuperBright rotating anode X-ray generator and high flux optics. For 10·5MeCN, one MeCN was refined as point atoms, the other four as regions of diffuse electron density using the Platon Squeeze procedure.¹³ Squeeze identifies 2 voids per unit cell, each containing 207 electrons. Inspection of the residual electron density prior to squeeze strongly suggested 4 MeCNs. Each MeCN contains 22 electrons so, although 207 electrons indicates *ca.* 9.4 MeCNs, only 8 were added per void, or 4 per metal complex. For 11·1 $\frac{3}{4}$ toluene·1 $\frac{1}{4}$ hexane, data were collected with an Agilent Gemini diffractometer using molybdenum radiation and an Eos S2 detector. Disordered solvent was modelled using the Squeeze routine, which identified two voids per unit cell containing a total of 1210 electrons. This was modelled using 9 toluene and 4 hexane molecules (the ratio of disordered toluene to hexane cannot be estimated by this technique).

Table 6 Crystallographic data for 7·2 $\frac{1}{4}$ MeCN, **8**, 9·4toluene, 10·5MeCN and 11·1.75toluene·1.25hexane

Compound	7·2 $\frac{1}{4}$ MeCN	8	9·4toluene	10·5MeCN	11·1.75toluene·1.25hexane
Formula	C _{59.50} H _{66.75} Al ₂ N _{6.25} O ₂	C ₅₄ H ₅₈ Al ₂ N ₄ O ₂	C ₁₀₈ H ₈₁ AlCl ₄ N ₈ O ₈	C ₁₁₄ H ₁₁₆ AlN ₁₃ O ₄	C _{264.50} H ₃₄₂ Al ₁₆ N ₁₆ O ₁₆
Formula weight	955.40	849.00	1787.58	1759.17	4433.20
Crystal system	Triclinic	Triclinic	Triclinic	Monoclinic	Triclinic
Space group	$P\bar{1}$	$P\bar{1}$	$P\bar{1}$	$P2_1/c$	$P\bar{1}$
Unit cell dimensions					
<i>a</i> (Å)	15.2938(19)	9.7916(5)	13.8593(10)	16.2328(2)	13.1640(3)
<i>b</i> (Å)	15.671(2)	11.2215(4)	14.7463(10)	27.3761(3)	31.8640(5)
<i>c</i> (Å)	25.086(3)	11.7840(6)	23.7238(17)	23.7006(3)	36.2145(5)
α (°)	93.9493(17)	84.624(4)	95.508(7)	90	113.2940(10)
β (°)	97.1008(16)	66.196(5)	101.879(7)	107.9523(6)	94.715(2)
γ (°)	112.5747(16)	84.347(4)	109.459(7)	90	95.712(2)
<i>V</i> (Å ³)	5464.4(12)	1176.81(10)	4401.9(6)	10 019.5(2)	13 759.6(4)
<i>Z</i>	4	1	2	4	4
Temperature (K)	150(2)	143(2)	143(2)	120.0(2)	120(2)
Wavelength (Å)	0.6884	0.71073	0.71073	0.71073	0.71073
Calculated density (g cm ⁻³)	1.161	1.198	1.343	1.166	1.072
Absorption coefficient (mm ⁻¹)	0.100	0.107	0.209	0.080	0.113
Transmission factors (min./max.)	0.987, 0.997	0.906, 1.000	0.514, 1.000	0.973, 0.990	0.564, 1.000
Crystal size (mm ³)	0.14 × 0.10 × 0.03	0.80 × 0.50 × 0.40	0.35 × 0.30 × 0.20	0.35 × 0.25 × 0.12	0.80 × 0.50 × 0.40
θ (max) (°)	22.6	26.4	27.4	25.0	29.5
Reflections measured	36 298	9795	67 195	191 662	155 744
Unique reflections	15 657	4806	20 011	17 619	64 526
<i>R</i> _{int}	0.065	0.023	0.067	0.105	0.051
Reflections with $F^2 > 2\sigma(F^2)$	9183	3428	12 308	13 161	43 448
Number of parameters	1319	283	1054	1095	2792
<i>R</i> ₁ [$F^2 > 2\sigma(F^2)$]	0.082	0.047	0.099	0.066	0.085
w <i>R</i> ₂ (all data)	0.263	0.127	0.291	0.153	0.255
GOOF, <i>S</i>	1.030	1.030	1.021	1.026	1.029
Largest difference peak and hole (e Å ⁻³)	0.76 and -0.32	0.45 and -0.35	0.90 and -0.51	0.28 and -0.29	1.44 and -0.59



Structures of the complexes **7–11** were solved using Direct Methods implemented within SHELXS-2013 and refined within SHELXL-2014.²⁴ Further details are provided in Tables 5 and 6.

Acknowledgements

Sichuan Normal University and the National Natural Science Foundation of China (grants 51273133 and 51443004) are thanked for financial support. The Special Funds for sharing large precision equipment (no. DJ2014-22) at Sichuan Normal University is also thanked. CR thanks the EPSRC for a travel grant (EP/L012804/1) and the National Crystallographic Service at the University of Southampton (for data collection of **9**-4toluene and **10**-5MeCN). The CCLRC is thanked for the award of beamtime (complex **7**-2₄MeCN) at SRS Daresbury Laboratory (Station 9.8), and the EPSRC Mass Spectrometry Service at Swansea is thanked for data.

References

- See for example: (a) E. M. Hodnet and J. W. Dunn, *J. Med. Chem.*, 1970, **13**, 768; (b) S. N. Pandeya, D. Sriram, G. Nath and E. De Clercq, *Il Farmaco*, 1999, **54**, 624; (c) A. H. El-Masry, H. H. Fahmy and S. H. Abdelwahed, *Molecules*, 2000, **5**, 1429; (d) A. A. Jarrahpour and M. Zarei, *Molbank*, 2004, M377; (e) H. L. Siddiqui, A. Iqbal, S. Ahmad and G. W. Weaver, *Molecules*, 2006, **11**, 206.
- (a) S. Brooker, *Coord. Chem. Rev.*, 2001, **222**, 33; (b) W. Radecka-Paryzek, V. Patroniak and J. Lisowski, *Coord. Chem. Rev.*, 2005, **249**, 2156.
- (a) F. H. Allen, *Acta Crystallogr., Sect. B: Struct. Sci.*, 2002, **58**, 380; (b) W. Yang, K.-Q. Zhao, B.-Q. Wang, C. Redshaw, M. R. J. Elsegood, J.-L. Zhao and T. Yamato, *Dalton Trans.*, 2016, **45**, 226–236.
- (a) A. Arbaoui, C. Redshaw and D. L. Hughes, *Chem. Commun.*, 2008, 4717; (b) A. Arbaoui, C. Redshaw and D. L. Hughes, *Supramol. Chem.*, 2009, **21**, 35.
- F. Majoumo-Mbe, E. Smolensky, P. Lönnecke, D. Shpasser, M. S. Eisen and E. Hey-Hawkins, *J. Mol. Catal. A: Chem.*, 2005, **240**, 91.
- R. Mazarro, I. Gracia, J. F. Rodriguez, G. Storti and M. Morbidelli, *Polym. Int.*, 2012, **61**, 265.
- P. Chakraborty, J. Adhikary, S. Samanta, I. Majumder, C. Massera, D. Escudero, S. Ghosh, A. Bauza, A. Frontera and D. Das, *Dalton Trans.*, 2015, **44**, 20032.
- Y. Wei, S. Wang and S. Zhou, *Dalton Trans.*, 2016, **45**, 4471.
- (a) S. R. Korupoju and P. S. Zacharias, *Chem. Commun.*, 1998, 1267; (b) S. J. Na, D. J. Joe, S. Sujith, W.-S. Han, S. O. Kang and B. Y. Lee, *J. Organomet. Chem.*, 2006, **691**, 611.
- (a) S. Brooker, G. S. Dunbar and T. Weyhermuller, *Supramol. Chem.*, 2001, **13**, 601; (b) J. Gao, J. H. Reibenspies, R. A. Zingaro, R. Woolley, A. E. Martell and A. Clearfield, *Inorg. Chem.*, 2005, **44**, 232; (c) S. J. Na, D. J. Joe, S. Sujith, W.-S. Han, O. S. Kang and B. Y. Lee, *J. Organomet. Chem.*, 2006, **691**, 611; (d) M. Paluch, J. Lisowski and T. Lis, *Dalton Trans.*, 2006, 381.
- (a) R. W. Stotz and R. C. Stoufer, *J. Chem. Soc., Chem. Commun.*, 1970, 1682; (b) J. D. O. Cabral, M. F. Cabral, M. G. B. Drew, F. S. Esho, O. Haas and S. M. Nelson, *J. Chem. Soc., Chem. Commun.*, 1982, 1066; (c) T. W. Bell and F. Guzzo, *J. Chem. Soc., Chem. Commun.*, 1986, 769; (d) T. Sato, K. Sakai and T. Tsubomura, *Chem. Lett.*, 1993, 859; (e) S. W. A. Bligh, N. Cho, V. W. J. Cummins, E. G. Evagoroula, D. J. Kelly and M. McPartlin, *J. Chem. Soc., Dalton Trans.*, 1994, 3369; (f) D. A. Plattner, A. K. Beck and M. Neuburger, *Helv. Chim. Acta*, 2002, **85**, 4000; (g) M. Allmendinger, P. Zell, A. Amin, U. Thewalt, M. Klinga and B. Rieger, *Heterocycles*, 2003, **60**, 1065; (h) J. Gregolinski, J. Lisowski and T. Lis, *Org. Biomol. Chem.*, 2005, **3**, 3161.
- A. Arbaoui, C. Redshaw and D. L. Hughes, *Chem. Commun.*, 2008, 4717.
- A. L. Spek, *Acta Crystallogr., Sect. A: Fundam. Crystallogr.*, 1990, **46**, C34.
- (a) J. M. Klerks, D. J. Stufkens, G. van koten and K. Vrieze, *J. Organomet. Chem.*, 1979, **181**, 271; (b) V. C. Gibson, C. Redshaw, A. J. P. White and D. J. Williams, *J. Organomet. Chem.*, 1998, **550**, 453; (c) M. Bruce, V. C. Gibson, C. Redshaw, G. A. Solan, A. J. P. White and D. J. Williams, *Chem. Commun.*, 1998, 2523; (d) V. C. Gibson, D. Nienhuis, C. Redshaw, A. J. P. White and D. J. Williams, *Dalton Trans.*, 2004, 1761; (e) V. C. Gibson, C. Redshaw, G. A. Solan, A. J. P. White and D. J. Williams, *Organometallics*, 2007, **26**, 5119; (f) A. Arbaoui, C. Redshaw and D. L. Hughes, *Supramol. Chem.*, 2009, **21**, 35; (g) W. Alkarekshi, A. P. Armitage, O. Boyron, C. J. Davies, M. Govere, A. Gregory, K. Singh and G. A. Solan, *Organometallics*, 2013, **32**, 249–259.
- (a) M. Shen, W. Zhang, K. Nomura and W.-H. Sun, *Dalton Trans.*, 2009, 9000; (b) M. Shen, W. Huang, W. Zhang, X. Hao, W.-H. Sun and C. Redshaw, *Dalton Trans.*, 2010, **39**, 9912; (c) M.-C. Chang, W.-Y. Lu, H.-Y. Chang, Y.-C. Lai, M. Y. Chiang, H.-Y. Chen and H.-Y. Chen, *Inorg. Chem.*, 2015, **54**, 11292.
- (a) N. Iwasa, S. Katao, J. Liu, M. Fujiki, Y. Furukawa and K. Nomura, *Organometallics*, 2009, **28**, 2179; (b) D. Li, Y. Peng, C. Geng, K. Liu and D. Kong, *Dalton Trans.*, 2013, **42**, 11295; (c) W.-L. Kong, Z.-Y. Chai and Z.-X. Wang, *Dalton Trans.*, 2014, **43**, 14470; (d) W. Zhang, Y. Wang, L. Wang, C. Redshaw and W.-H. Sun, *J. Organomet. Chem.*, 2014, **750**, 65.
- C. Redshaw, M. A. Rowan, L. Warford, D. M. Homden, A. Arbaoui, M. R. J. Elsegood, S. H. Dale, T. Yamato, C. Pérez-Casas, S. Matsui and S. Matsuura, *Chem. – Eur. J.*, 2007, **13**, 1090–1107.
- T. K. Sen, A. Mukherjee, A. Modak, S. K. Mandel and D. Koley, *Dalton Trans.*, 2013, **42**, 1893.



- 19 (a) R. S. Drago, M. J. Desmond, B. B. Corden and K. A. Miller, *J. Am. Chem. Soc.*, 1983, **105**, 2295; (b) J. J. Randell, C. E. Lewis and P. M. Slangen, *J. Org. Chem.*, 1962, **27**, 4098.
- 20 V. C. Gibson, C. Redshaw, W. Clegg, M. R. J. Elsegood, U. Siemeling and T. Türk, *Polyhedron*, 2004, **23**, 189.
- 21 *SMART and SAINT software for CCD diffractometers*, Bruker AXS Inc., Madison, USA, 2001 and 2007.
- 22 G. M. Sheldrick, SHELX-97 – Programs for crystal structure determination (SHELXS) and refinement (SHELXL), *Acta Crystallogr., Sect. A: Fundam. Crystallogr.*, 2008, **64**, 112–122.
- 23 *Programs CrysAlis-CCD and -RED*, Oxford Diffraction Ltd., Abingdon, UK, 2005.
- 24 G. M. Sheldrick, *Acta Crystallogr., Sect. C: Cryst. Struct. Commun.*, 2015, **71**, 3–8.

